Limit-Analysis of R/C slabs exposed to standard fires: application of the Yield-line method

Structural Engineering Department.

ELIAS YUSUF ALI

POLITECNICO DI MILANO, ITALY

October, 2010.

Limit-Analysis of R/C slabs exposed to standard fires: application of the Yield-line method

A Thesis submitted to Structural Engineering Department, Politecnico Di Milano, in partial fulfillment of the requirements for the degree of Master of Science in Civil Engineering.

October 2010, ITALY

ELIAS YUSUF ALI

Politecnico Di Milano

Structural Engineering Department

Email: eliasyus_2006@yahoo.com

Tel. +393898754783

Guidance and supervision by:

Prof. Pietro Gambarova

Politecnico Di Milano

Structural Engineering Department

Email: gamba@stru.polimi.it

A Thesis submitted to Structural Engineering Department, Politecnico Di Milano, in partial fulfillment of the requirements for the degree of Master of Science in Civil Engineering.

October 2010, ITALY

Acknowledgements

I am heartily thankful to my supervisor, Prof. Pietro Gambarova, whose encouragement, guidance and support from the initial to the final level enabled me to develop an understanding of the subject.

Lastly, I offer my regards and blessings to my family, friends and all of those who supported me in any respect during the completion of the thesis and during my stay in Italy.

Elias Yusuf Ali

Contents

NOTATIONS

Greek letters

γ_G	[ ]	partial loading factor for permanent actions.
γ_G	[ ]	partial loading factor for variable actions.
γ_s	[ ]	partial safety factor for reinforcement.
γ_c	[ ]	partial safety factor for concrete.
ρ_o	[ ]	reference reinforcement ratio.
ρ	[ ]	required tension reinforcement ratio
ρ'	[ ]	required compression reinforcement ratio
θ	[ ]	relative rotation between the segments of the yield line
α, β	[ ]	relative positions of the yield line for the two mechanisms
λi	[ ]	ration of moments ($\frac{Mx^+}{My^+}$)
α_{cc}	[ ]	partial safety factor to take in to account long term loading
α_{ct}	[ ]	partial safety factor to take in to account long term loading
$\emptyset$	[mm]	reinforcement diameter
$\delta \; or \; \Delta$	[mm]	downward deformation of the centroid
λ	[W/mK]	thermal conductivity
$\rho(\theta)$	[Kg/m^3]	concrete density as a function of temperature
σ_c	[N/mm^2]	compressive stress

Alphabetical letters

A	[m2]	total area of the compartment
A_f	[m2]	area of the floor
A_t	[m2]	total area of the enclosure

A_v	[m2]	total area of vertical openings
a	[m]	length of the slab
b	[m]	length of the slab
c_{min}	[mm]	minimum cover for durability requirement for the reinforcement
D	[cm]	depth of the slab
d’	[mm]	effective depth
E	[J]	total energy that could theoretically be released in the compartment fire
E_{cm}	[N/mm2]	secant modulus
Hc_i	[J/kg]	heat of combustion of each items present in the compartment
M_i	[kg]	the mass of each items present in the compartment
m_x	[kNm]	bending moment on the x-face of the slab
m_y	[kNm]	bending moment on the y-face of the slab
m_{xy}	[kNm]	twisting moment on the x-face of the slab in y direction
m_{un}	[kNm]	ultimate moments of resistance on the yield line pattern
p_{xy}	[kN/m2]	total distributed load on the slab
r	[kN/m2/m]	distributed load on the strip per unit length of the slab
R	[kN/m]	resultant concentrated load per unit length of the slab
SS	[ ]	simple support
CL	[ ]	clamped (fixed) support
v_y	[kN]	shear force acting on the x-face of the slab
v_x	[kN]	shear force acting on the y- face of the slab
w_u	[kN]	total load on the segment of the yield line

Chapter 1
INTRODUCTION

1.1 ABSRTACT

With the increased incidents of major fires and fire accidents in buildings, design, assessment, repair and rehabilitation of fire damaged structures has become a topical interest. This specialized field involves expertise in many areas like concrete technology, materials science and testing, structural engineering, repair materials and techniques etc.

In this thesis work, a thin R/C slab resting on beams on the three sides and free edge on the remaining side with an area of $48m^2$ is studied. The slab is first analyzed and designed for room temperature, then it is also studied to observe the behavior and stress distribution when the slab is exposed to three different fire conditions: **real fire scenario, standard fire(ISO-834).**

Limit analysis according to Yield-Line method is applied to identify the weakest resistant mechanisms among the several global and local mechanisms, that are kinematically admissible for the given restraints, loads and fire conditions of the slab.

Estimation of temperatures, modulus of elasticity and strength in the post-flashover fires on concrete and reinforcement is an essential part of the analysis and design of the considered slab, in order to verify that the fire resistance of the slab is greater than the severity of the fires to which the slab is exposed.

The behavior of structures exposed to fire is usually described in terms of fire resistance, which is the period of time under exposure to a standard fire at which some requirements are to be met. In performance-based design these requirements may be defined as structural collapse or loss of integrity (which allows fire-spread to occur), but is more usually defined in terms of limit deflections.

The objective of fire safety is to protect life and property. Fires can occur at any time in buildings, and the safety of occupants and maintaining the integrity of the structure are of major importance. Building codes prescribe detailed measures for the fire safety of structural members because when other means for containing a fire fail, such as a fire suppression system ,structural integrity is the last line of defense. Code-based structural fire safety requirements refer to fire resistance which is defined as the ability of a structural element to maintain its load-bearing functions under fire conditions.

The fire resistance rating of a structural member is the elapsed time it exhibits resistance with respect to structural integrity, stability, and temperature transmission while exposed to standard fire conditions. The measured fire resistance of a structural member or assembly is dependent on the geometry of elements, materials used in construction, load intensity and fire exposure.

Testing for the fire resistance of materials is done in laboratories by exposing elements to fire conditions and monitoring their performance. Numerical and analytical methods were developed based on these fire tests as an economical alternative to laboratory testing. Over the past two decades there has been a widespread use of finite element programs to determine structural performance in both standard and natural fire conditions.

The above methods for predicting fire resistance do not increase the awareness of structural engineers to the concepts of design for fire conditions. They are either prescriptive in their application to design or being performed by the materials and fire communities whose interests are geared towards properties of materials in fire conditions and complicated performance-based analyses of structural elements. From a design standpoint it is not sensible for a practicing

structural engineer to use finite element software to analyze structural fire performance because analyses are time consuming and the use of these programs requires a strong background in fire protection engineering which most structural engineers do not have.

The motivation for this thesis was to increase the awareness of the structural engineering field to the concepts behind structural design for fire safety using simplified design tool, ***limit-analysis***, that predict the fire performance of structural elements, which is of utmost importance to practicing structural engineers.

1.2 Objectives of this thesis work

In this paper, it is tried to show the application of the yield-line method how powerful and easy for design and analysis, by considering the different fire conditions on the slab.

The main discussions are:

1. Design of the slab using the strip-method.
2. Evaluating the collapse load of the slab using the yield-line method
3. Evaluating the time-temperature for the slab when exposed to the standard fire, and standard fire resistance is calculated, i.e the ability of the slab to fulfill the required functions, for the exposure of heating according to the standard temperature-time curve for the specified load combination and for the stated period of time (EN-1991-1-2)
4. Evaluating the time-temperature of the slab during real fire-scenario using (ABAQUS) and determining once again the resistance of the slab for this fire condition using the yield-line method.
5. Comparing the fire resistance of the slab for the above fire situations and provide the possible collapse mechanism.

1.3 EXPERIENCE OF FIRES:

Annual statistics on losses caused by fires in homes and elsewhere make for some unpleasant readings, but these events make it possible learn more about fire-safety design.

We are all aware of the damage that fire can cause in terms of loss of life, homes and livelihoods. A study on 16 industrialized nations (13 in Europe plus the USA, Canada and Japan) found that, in a typical year, the number of people killed by fires was 1 to 2 per 100,000 inhabitants and the total cost of fire damage amounted to 0.2% to 0.3% of GNP. The loss of business resulting from fires in commercial and office buildings runs into millions of Euros each year. The extent of such damage depends on a number of factors such as building design and use, structural performance, fire extinguishing devices and evacuation procedures. (*Reproduced from The Office of the Fire Marshal (OFM),Ontario, Canada*.)

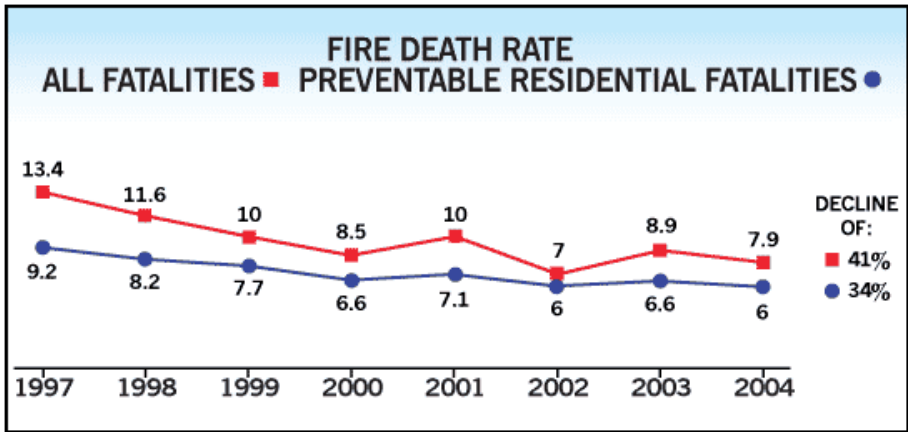

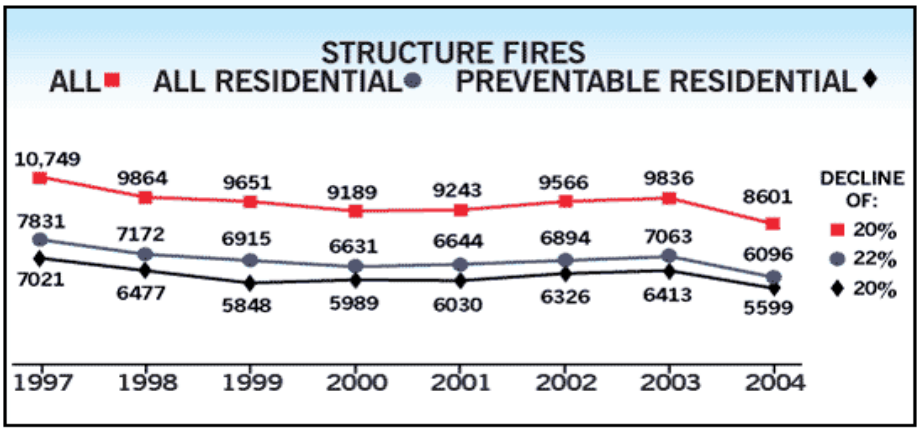

1.4 Development of Fire in enclosures

Development of fire in a room can be divided in several phases (figure 2)

1. First one is the **ignition** of the fire. As it is the first step of any compartment fire, ignition is probably the most important phenomenon: without ignition, there is no fire. Many studies have been conducted on this subject, leading to wide variety of test methodologies to evaluate the potential of being ignited that a material has. Babrauskas (2001) reports that ignition temperature of wood exposed to the minimum heat flux possible for ignition is around 250°C. The surface temperature of fuel is usually considered to be the best empirical parameter to describe the ignition of fuel, nevertheless the temperature of the environment in which the fuel is presented is usually preferred.
2. Then comes the **propagation** or **Growth** phase, during which fire spreads. Some combustible gases are rising towards the ceiling, a fire plume is forming above the fire source. Some air is entered in the fire plume and a hot smoke layer is forming in the upper part of the compartment leaving the clear in the lower part (figure 1). The temperature rise in the compartment and ,from here, the situation can evolve towards one of the two following possibilities:
    - Either the temperature of the gases become so elevated that, after a certain period of time, it causes the sudden ignition of every object in the compartment. This phenomenon is called the **flashover**. After the flashover time, **there is a fully developed fire**.
    - Either there is no spread of the fire to the whole compartment, because the propagation is so slow that the temperature rise is not sufficient to cause the flashover, or the fire can find no combustible material in its close vicinity, thus the fire remains **localized**.

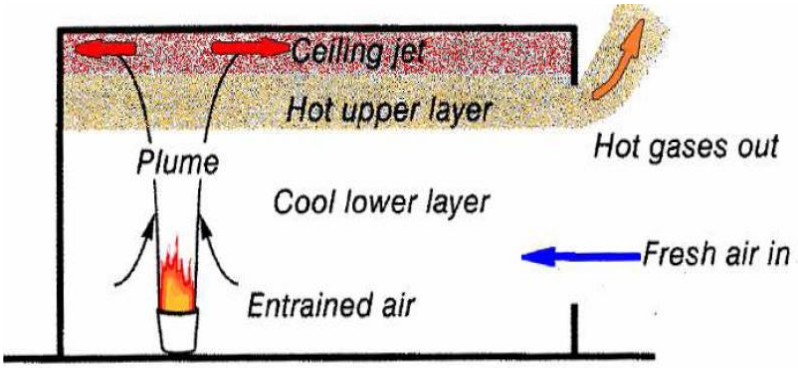

Figure:1 pre-flash over fire

3. In the next period, the fire is **fully developed , i.e.** the fire keeps on burning at a rather constant rate, leading to small variation of the temperatures.
4. The last phase is the **cooling phase** or **decay** phase.

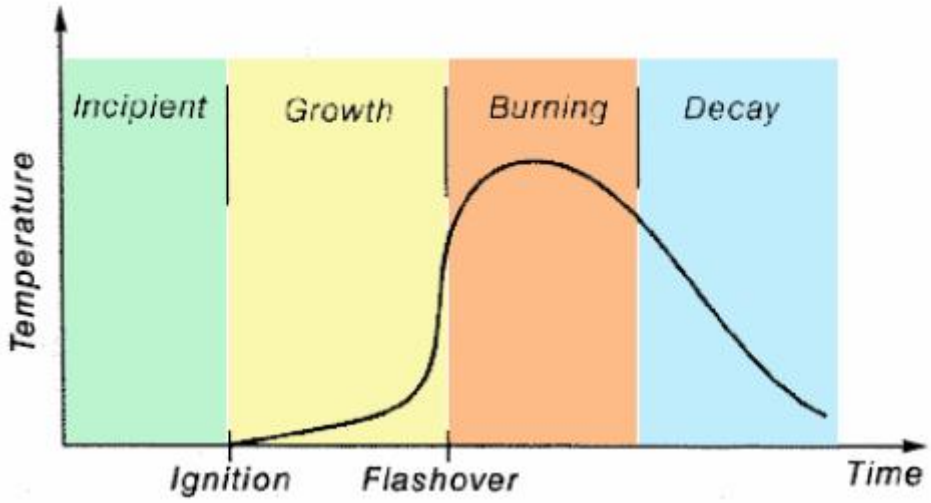

Figure:2 process of fire development

The ignition and the propagation phases of the fire depend mainly on the fuel characteristics because oxygen is usually widely available during these phases.

The period up to flashover is often called **pre-flashover** fire phase during which the fire is usually localized. After flashover, the fire phase is called **post-flashover**. A post-flashover fire is a fully developed fire if combustible material is present. On the other hand, the amount of ventilation has big influence during the fully developed phase of the fire.

Two situations are possible:

- The ventilation is large enough to have no influence on the fire source development. There is sufficient oxygen available for combustion. The fire is said to be fuel controlled because the heat released in the compartment depends mainly on the characteristics of the material that is burning.
- The ventilation is small, considering the size of the fire, and there is not enough oxygen to combust all the fuel. The fire is said to be ventilation controlled because the rate of heat release in the compartment depends mainly on the amount of available oxygen and therefore on the ventilation conditions.

In most cases, localized/pre-flashover fires are fuel controlled and fully developed/post-flashover fires are ventilation controlled.

1.5 Fire Load

The fire load in a compartment is defined as the total energy that could theoretically be released in the compartment in case of fire. It consist of the different elements present in the compartment (for our case library with furniture, books, etc), of the construction elements, of partition linings and in general, of all the combustible content.

The fire load is usually expressed in Joules and is the sum of the product of the mass *Mi* of each items present in the compartment by its heat of combustion *Hc,i.* (Eq1)

$$E=M_i*H_{c,i} \quad \text{……..(Eq.1)}$$

Chapter 2

LIMIT ANAYISIS OF SLABS.

2.1 Introduction.

The complexities involved in obtaining a progressive failure solution to a reinforced concrete problems, which includes the effect of cracking, bond slips, dowel action and aggregate interlock, requires a simple methods to be adopted in order to assess the load carrying capacity in a more direct manner without carrying out a complete progressive-failure analysis of stress and strains in the slab. Thus, limit-analysis plays a major role in this end.

Applications of limit-analysis to reinforced concrete structures have not been as extended as for steel frame structures, but the method has been successfully applied in the analysis of reinforced concrete structures. For reinforced concrete slabs with a load acting perpendicular to their plan, there is the yield-line theory developed by Ingerslev (1921, 1923), Johansen(1943), and Gvozdev(1938) and Prager. Limit-analysis based on yield-lines has been applied to reinforced concrete slabs and disks by Nielsen (1964, 1971).

The two theorems of limit- analysis as stated by Prager are:

2.1.1 Upper-bound Theorem

> "*A kinematically admissible deformation field in a rigid-plastic continuum will be unstable when the work done by the applied loads is greater than the energy dissipated by the yield mechanism. This means that the resistance calculated for the kinematically-admissible mechanism will be greater than or equal to the required resistance and plastic flow will occur*."

2.1.2 Lower-bound Theorem

"*Plastic flow will not occur in a rigid plastic continuum with a stable stress field. The resistance calculated with this stress field will be smaller than or equal to that required for collapse."*

For a lower bound solution a distribution of moments for the whole plate is found such that:

1. The equilibrium conditions are satisfied at all the points in the plate.
2. The yield criterion defining the strength of the slab elements is not exceeded anywhere in the slab.
3. The boundary conditions are complied with.

Limit analysis based on such theories indicates that exact solutions for plates are not always possible. In general, the calculated ultimate (collapse) load lies between the two limits, depending upon the approach adopted.

In the following chapters, we will apply the two theorems for the typical slab we are dealing with.

2.2 Building Description

The building studied in this paper is a library with its floor area as shown below in Figure 3.The height of the floor is 3.50 m and the size of the rectangular floor plan is 8 m x 12 m. The building has three identical windows on two adjacent walls and also one fire resistant door.

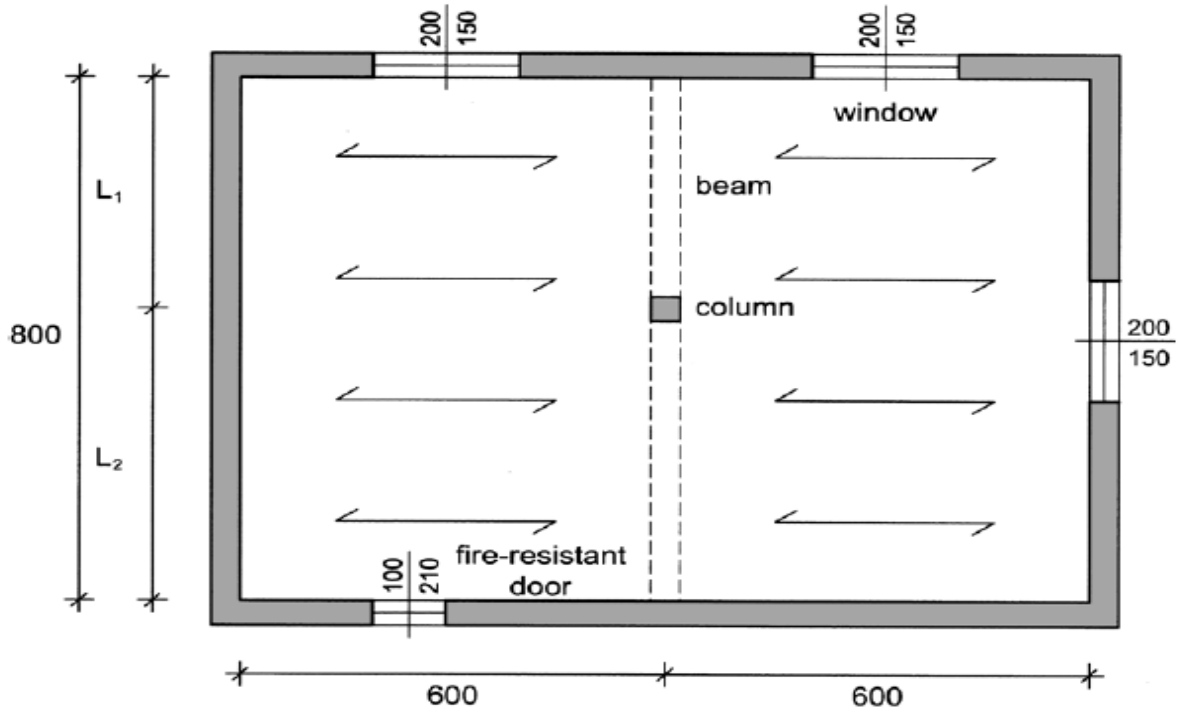

Figure3 . General Floor Area (plan) of Library building.

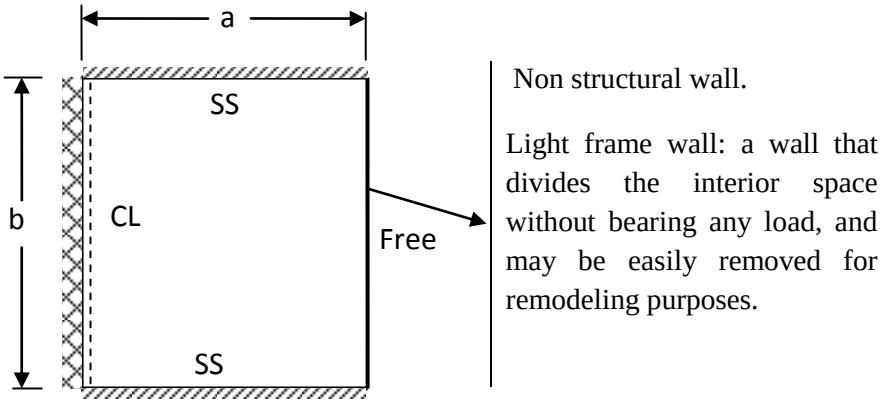

Fig: 4 Boundary conditions for the slab under study.

2.2.1 Minimum depth requirement for the slab.(EN1992-1-1)

The thickness of a floor slab must be determined in an early phase of design because the weight of the slab is an important part of the dead load of the structure. The minimum thickness can be determined by many factors:

- Shear strength of beamless slabs (usually a controlling factor); slab must be thick enough to provide adequate shear strength
- Flexural moment requirement (less often a governing factor)
- Fire-resistance requirements
- Deflection control (most common thickness limitations)

The deformation of the slab considered shall not be such that it adversely affects its proper functioning or appearance. Appropriate limiting values of deflection taking into account the nature of the structure, of the finishes, of the partitions and of the fixings.

Generally, it is not necessary to calculate the deflections explicitly, as simple rules are given in the technical literatures. (For example limiting the span/depth ratio) are available. which will be adequate for avoiding deflection problems in normal circumstances. More rigorous checks are necessary for members which lie outside such limits, or where deflection limits other than those simplified in simplified methods are appropriate.

Provided that reinforced concrete beams or slabs in buildings are dimensioned so that they comply with the limits of span to depth ratio given in the code, their deflections may be considered as not exceeding the limits set out in (EN1992-1-1). The limiting span/depth ratio may be estimated using expressions (Eq.2.a) and (Eq.2b) and multiplying this by correction factors to allow for the type of reinforcement used and other variables. No allowance has been made for any pre-camber in the derivation of these expressions.

$$\frac{l}{d} = K\left[11 + 1.5\sqrt{f_{ck}}\frac{\rho_o}{\rho} + 3.2\sqrt{f_{ck}}\left(\frac{\rho_o}{\rho} - 1\right)^{3/2}\right] \quad if\ \rho \le \rho_0 \text{.....(Eq. 2a)}$$

$$\frac{l}{d} = K\left[11 + 1.5\sqrt{f_{ck}}\frac{\rho_o}{\rho - \rho'} + \frac{1}{12}\sqrt{f_{ck}}\sqrt{\frac{\rho'}{\rho_0}}\right] \qquad if\ \rho > \rho_0 \text{.....(Eq.2b)}$$

where:

- l/d is the limit value of the span/depth
- K is the factor to take into account the different structural systems
- ρ_0 is the reference reinforcement ratio = $\sqrt{f}$ck 10^{-3}
- ρ is the required tension reinforcement ratio at mid-span to resist the moment due to the design loads (at support for cantilevers)
- ρ' is the required compression reinforcement ratio at mid-span to resist the moment due to design loads (at support for cantilevers)
- f_{ck} is the compressive characteristic strength in MPa units

Expressions (2.a) and (2.b) have been derived on the assumption that the steel stress, under the appropriate design load at SLS at a cracked section at the mid-span of a slab or at the support of a cantilever, is 310 MPa (corresponding roughly to f_{yk} = 500 MPa).

Note: Values of K for use in a country may be found in its National Annex. Recommended values of K are given (EN1992-1-1 Table 7.4N). Values obtained using expression (Eq.2) for common cases (C30, σ_s = 310 MPa, different structural systems and reinforcement ratios ρ = 0,5 % and ρ = 1,5 %) are also given.

Table 7.4N: Basic ratios of span/effective depth for reinforced concrete members without axial compression

Structural System	K	Concrete highly stressed ρ = 1,5%	Concrete lightly stressed ρ = 0,5%
Simply supported beam, one- or two-way spanning simply supported slab	1,0	14	20
End span of continuous beam or one-way continuous slab or two-way spanning slab continuous over one long side	1,3	18	26
Interior span of beam or one-way or two-way spanning slab	1,5	20	30
Slab supported on columns without beams (flat slab) (based on longer span)	1,2	17	24
Cantilever	0,4	6	8

Note 1: The values given have been chosen to be generally conservative and calculation may frequently show that thinner members are possible.
Note 2: For 2-way spanning slabs, the check should be carried out on the basis of the shorter span. For flat slabs the longer span should be taken.
Note 3: The limits given for flat slabs correspond to a less severe limitation than a mid-span deflection of span/250 relative to the columns. Experience has shown this to be satisfactory.

The slab considered in our case is categorized as: two-way spanning slab of continuous over one long side; hence: l/d=26

which means: d=600/26=23.08cm

That has been increased to 30cm to take care of possible cracking.

2.2.2 Minimum concrete cover

According to EN 1992-1-1, values of c_{min} depends on the structural classification and environmental exposure condition for the steel and the concrete. The min value can be found in national annexes. The recommended Structural Class (design working life of 50 years) is S4. The

Table 4.4N: Values of minimum cover, $c_{min,dur}$, requirements with regard to durability for reinforcement steel in accordance with EN 10080.

Environmental Requirement for $c_{min,dur}$ (mm)							
Structural Class	**Exposure Class according to Table 4.1**						
	X0	XC1	XC2 / XC3	XC4	XD1 / XS1	XD2 / XS2	XD3 / XS3
S1	10	10	10	15	20	25	30
S2	10	10	15	20	25	30	35
S3	10	10	20	25	30	35	40
S4	10	15	25	30	35	40	45
S5	15	20	30	35	40	45	50
S6	20	25	35	40	45	50	55

recommended minimum Structural Class is S1

Thus, for the slab under consideration for structural class S4 and exposure class XC2

minimum concrete cover c_{min}=25mm.

- concrete cover used: 30mm

2.2.3 Material properties:

Concrete strength: C30/37

Characteristic compressive strength on cylinder $f_{ck} = 30N/mm2$

Design compressive strength (EC2) $f_{cd} = \alpha_{cc}\frac{f_{ck}}{\gamma_c} = 0.85 * \frac{30}{15} = 17N/mm2$

Average value of tensile strength $f_{ctm} = 0.3\ (f_{ck})^{2/3} = 2.896\ \mathrm{N/mm2}$

Secant modulus $E_{cm} = 22[(fck + 8)/10]^{0.3} = 32836\ \mathrm{N/mm2}$

- γc = is the partial safety factor for ultimate limit state for concrete and is γc = 1.5.
- αcc = is the factor that takes into account the effects of loads on the long-term resistance and adverse effects resulting from the manner in which the load is applied: αcc = 0.85
- αct= factor that takes into account the effects of loads on the long-term resistance traction and adverse effects resulting from the manner in which the load is applied: αct = 1.0

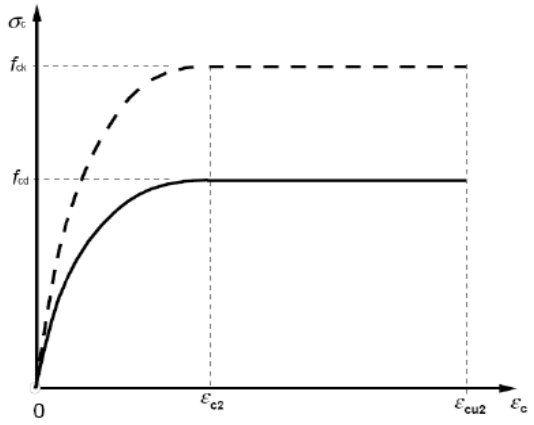

Fig:5 Parabola-rectangle diagram for concrete in compression.

Yield strength of steel: 500

Characteristic yield strength…. $f_{yk} = 500\ N/mm^2$

Design yield strength (EC2)

$$f_{yd} = \frac{f_{yk}}{\gamma_s} = \frac{500}{1.15} = 435\ N/mm^2$$

Modulus of elasticity (EC2) $E_s = 200000\ N/mm^2$

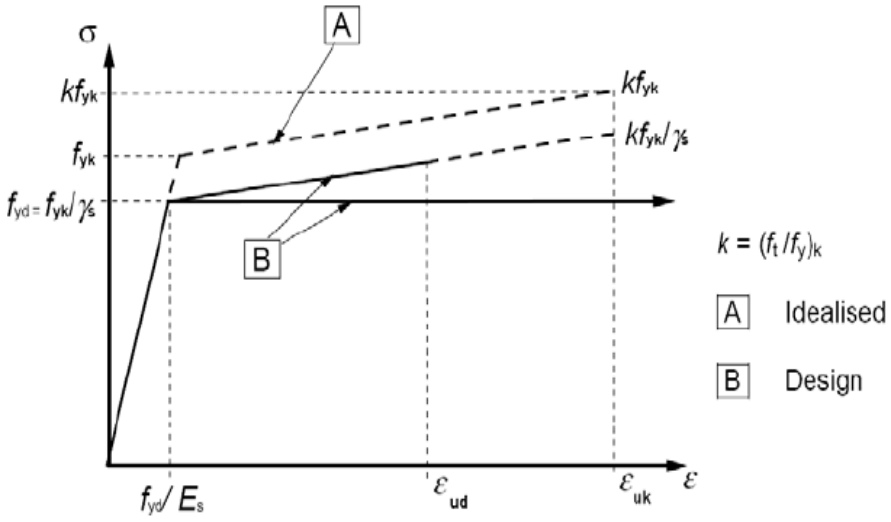

Fig:6 Idealized and design stress-strain diagrams for reinforcing steel (for tension and compression)

Chapter 3

DESIGN OF REINFORCEMENTS USING THE STRIP METHOD

The Longitudinal reinforcement is designed by applying the Strip Method. The Strip Method is based on the lower bound theorem of the theory of plasticity. This means that the solution obtained are on the safe side, provided that the theory of plasticity is applicable, which is the case for bending failures in our slab with ordinary reinforcement, concrete and normal proportions of the reinforcement. The lower bound design method for reinforced concrete slabs suggested by Hilleborg in 1956 can be stated as:

" If a distribution of moments can be found which satisfies both the equilibrium and the boundary conditions for a given external load, and if the plate is at every point able to carry these moments, then the given external load will represent a lower limit of the carrying capacity of the plate."

3.1 Governing Equations For General Lower-Bound Limit Analysis.

Equilibrium Equation

Consider the equilibrium of a small element with sides *dx* and *dy* taken from the slab and let *p* be the external load acting on the element per unit area, as shown in the figure.

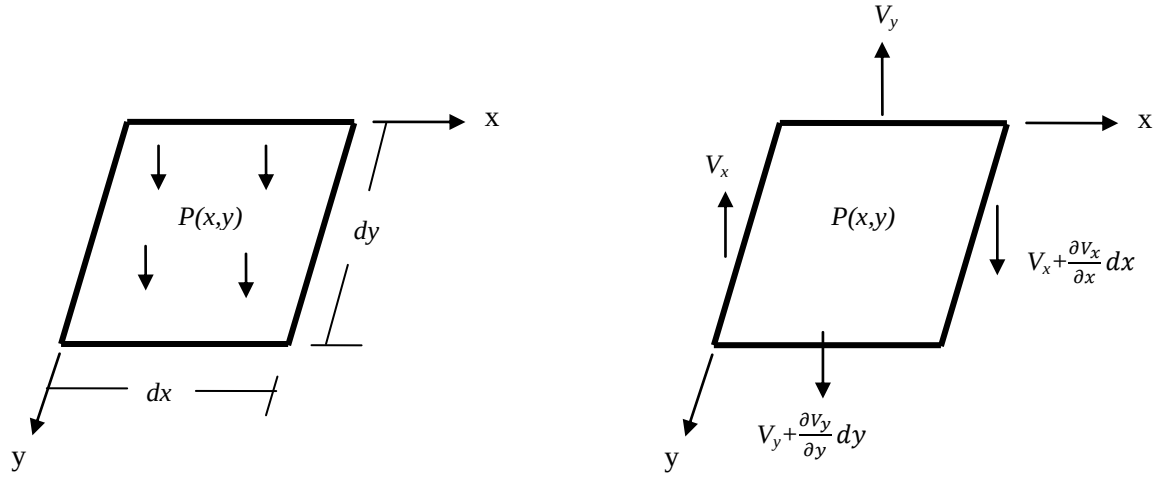

The shear forces per unit width V_x and V_y, the bending moments per unit width, m_x and m_y and the twisting moments per unit width, m_{xy} and m_{yx} acting on the faces of the element in the x- and y- directions are also shown in the figure below.

From the equilibrium of the vertical forces:

$$\left(V_x + \frac{\partial V_x}{\partial x}dx\right)dy + \left(V_y + \frac{\partial V_y}{\partial y}dy\right)dx - V_x dy - V_y dx + p dx dy = 0 \text{…….(Eq. 3)}$$

$$\frac{\partial V_x}{\partial x} + \frac{\partial V_y}{\partial y} = -p$$

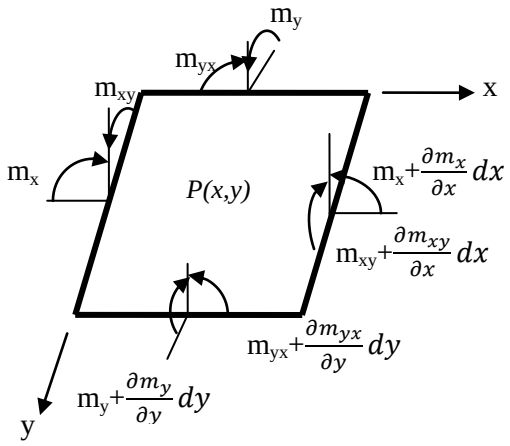

From the equilibrium of moments about the y-direction axis passing through the center of the element and ignoring higher-order terms:

$$\left(2V_x + \frac{\partial V_x}{\partial x}dx\right)dy\frac{dx}{2} - \frac{\partial m_x}{\partial x}dx\,dy - \frac{\partial m_{xy}}{\partial y}dx\,dy = 0 \text{……..(Eq.4)}$$

$$\frac{\partial m_x}{\partial x} + \frac{\partial m_{xy}}{\partial y} = V_x$$

Similarly, from the equilibrium of moments about an x-direction axis passing through the center of the element:

$$\frac{\partial m_y}{\partial y} + \frac{\partial m_{xy}}{\partial x} = V_y$$

Substituting the above equations gives:

$$\frac{\partial^2 m_x}{\partial x^2} + 2\frac{\partial^2 m_{xy}}{\partial x \partial y} + \frac{\partial^2 m_y}{\partial y^2} = -p(x,y) \text{.....(Eq.5)}$$

The above equation (Eq. 5) is based on the static theorem of limit analysis, so that each part of the structure and the overall structure must be in equilibrium with the loads applied. Bending moments must respect the flexural equilibrium.

Hilleborg has also simplified the general lower bound method for slab design by eliminating the twisting moments when deriving the design moments. If no external load is required to be carried by torsion, we can treat the slab as if composed of a system of strips, generally in two directions at right angles, which enable the design moment to be calculated by simple statics involving the equilibrium of the strips.

Because the aim of the Strip method is the design of the reinforcement, it is advisable not consider the torsion, as the mechanisms related to it are not totally controlled by the designer. In this way the hypothesis means that the slab involves a set of strips, along the two directions, each subjected to bending and shear. Neglecting the twisting components, the above equation (Eq.5) can be simplified as follows:

$$\frac{\partial^2 m_x}{\partial x^2} + \frac{\partial^2 m_y}{\partial y^2} = -p(x,y) \text{.....(Eq. 6)}$$

The above equation stands that if we consider a coefficient α between 0 and 1, the strips along x carry a load equal to αp, while the strips along y carry a load equal to (1-α)p.

$$\frac{\partial^2 m_x}{\partial x^2} = -\alpha p$$

$$\frac{\partial^2 m_y}{\partial y^2} = -(1-\alpha)p \ldots\ldots\ldots\ldots .where\ 0 < \alpha \leq 1$$

Based on these considerations the slab will be subdivided into a limited number of strips, each subjected to a different distributed load, depending on the position of the strips with respect to the boundaries. As a matter of fact, the choice of α is done on the basis of the more effective mechanism to transmit the load.

For the slab studied in this paper, the subdivision is proposed in Figure 7, where the numbers stand for the values of α. Near a fixed edge the coefficient is high, while near a free edge α tend to zero, because there is no possibility to transmit the load in the x direction. For the other strips the values are intermediate.

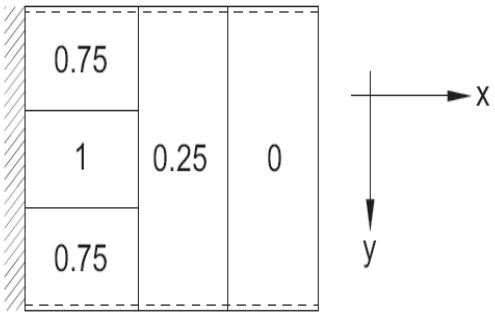

Fig:7 Distribution of α for the slab studied.

3.2 Load combination on the slab

Uniform load comes from the self weight of the slab and from the variable load:

Permanent load=12kN/m2

Variable load=3kN/m2

According to EN-1990, combination of action to obtain the design distributed load:

Partial loading factor for permanent actions $\gamma_G = 1.35$ (EN 1990 Table A1)

Partial loading factor for variable actions $\gamma_Q = 1.5$(EN 1990 Table A1)

$$P\left(\frac{kN}{m^2}\right) = 1.35G_k + 1.5Q_k = 22.05kN/m2$$

Fire limit state design loads.

For fire limit state, partial loading factors (γ_i) are not applied to either permanent actions or variable actions. Thus

$$q_{fire}\left(\frac{kN}{m^2}\right) = 1.0G_k + 1.0Q_k = 15kN/m2$$

3.3 Reinforcement calculations

- Dimension a=6m, b=8m
- $a' = 40\%a = 2.4m$
- $a'' = a''' = 30\%a = 1.8m$
- $b' = b'' = b''' = \frac{b}{3}$

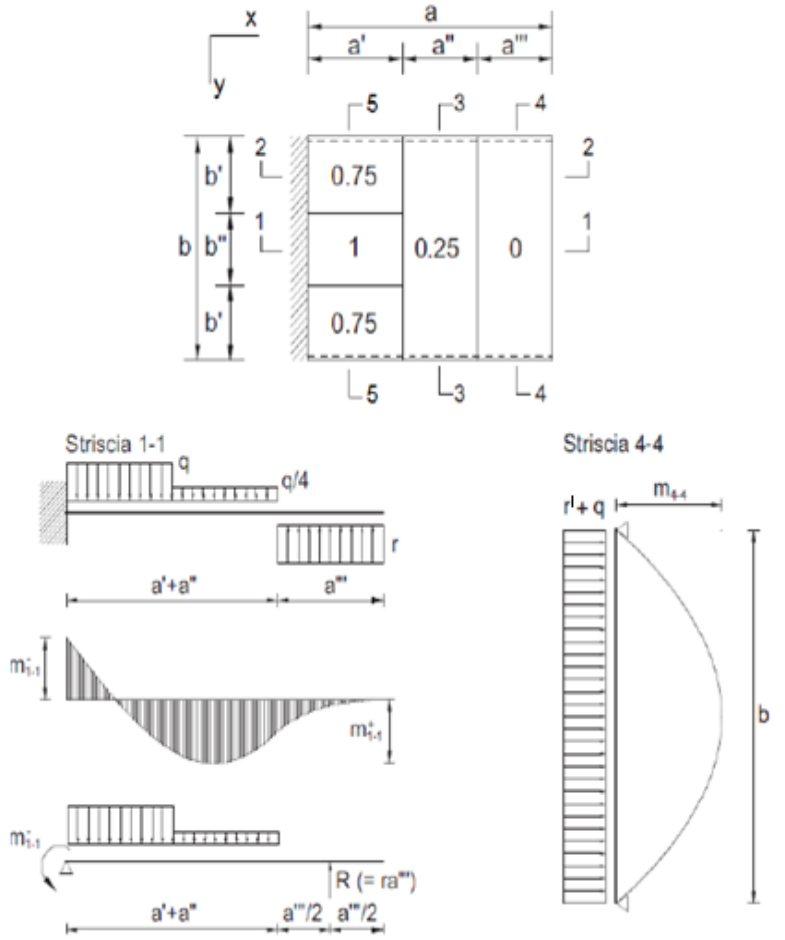

Fig:8 static scheme for the design of reinforcement for strip1-1 and strip 4-4

Design bending moment diagrams.

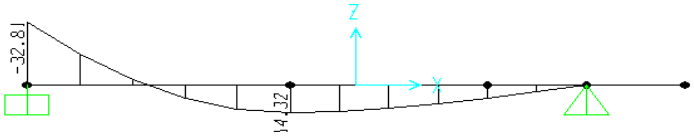

moment diagram along strip 1-1(see Fig.8)

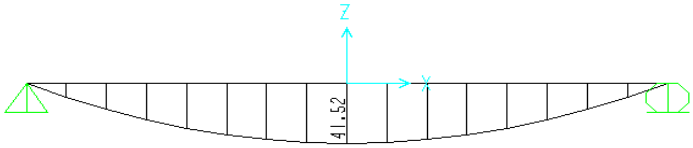

moment diagram along strip 4-4(see Fig.8)

Negative and positive moments referred to strip 1-1 are evaluated considering a cantilever with length 'a', subjected to a distributed load q and q/4, but also to a distributed load r. This load is present because near the free edge there exists the effect of the orthogonal strip, which is greater than the effect of the fixed edge. So the load r acts also on the strip 4-4, where the static scheme is that of a simply supported beam. Actually load r acts only on the strip1-1, because for the external ones the load would be r' < r, considering the smaller coefficient α near the fixed edge for strip 2. The choice to use the value r for the entire length is on the safe side.

$$R = r.a''' = 8.62KN$$

$$r = \frac{R}{a'''} = \frac{8.62}{1.8} = 4.79KN/m \ldots \text{on strip 1-1}$$

But when we consider the strip 4-4 the value of "r" should be adjusted with respect to the actual distributed length, which is b''.

$$r' = \frac{R}{b''} = \frac{8.62}{2.67} = 3.23KN/m \ldots \text{on strip 4-4}$$

The value of r (or R = $r.a'''$) depends, through equilibrium considerations, only from the value of the negative moment $m^{-}{}_{1-1}$. In this way we have the possibility to set this value, considering that the choice influences the value of $m^{+}{}_{1-1}$and $m^{+}{}_{4-4}$.

Positive and negative moments for the two critical sections considered are evaluated as:

$$m^{-}{}_{x} = m^{-}{}_{1-1} = 32.813\, {}^{kNm}/_{m}$$

$$m^{+}{}_{x} = m^{+}{}_{1-1} = 14.32\, {}^{kNm}/_{m}$$

$$m^{+}{}_{y} = m^{+}{}_{4-4} = 141.516\, {}^{kNm}/_{m}$$

Considering for each strip a section of unit length , the minimum reinforcement A_s is chosen imposing two equilibrium equations, one for the translation and the other for the rotation, and can be obtained as:

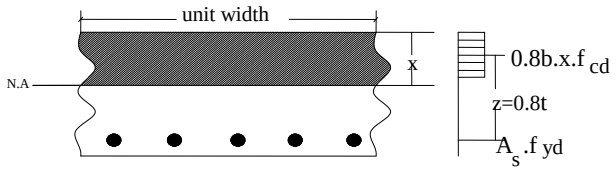

$$A_s = \frac{m_{i-i}}{o.8.t.f_{yd}} \text{.....(Eq.7)}$$

Using (Eq.7) and ϕ16 diam. bar: $A^{+}{}_{y} = \frac{m_{4-4}}{o.8.t.f_{yd}} = 2998mm^2/m.$

$$A^{+}{}_{x} = \frac{m^{+}{}_{1-1}}{o.8.t.f_{yd}} = 267mm^2/m$$

$$A^{-}{}_{x} = \frac{m^{-}{}_{1-1}}{o.8.t.f_{yd}} = 644mm^2/m$$

$$A^{-}{}_{y} = 0.2A^{+}{}_{y} = 600mm^2/m$$

In the analysis with the yield-line method, it is useful to express all the moments as a ratio of the reference moment. Here the choice is to consider $m^+{}_y$ as the reference moment, in the next sections called simply $m^+{}_y$:

$$m^+{}_x = \lambda_1 m^+{}_y = 0.101 m^+{}_y$$

$$m^-{}_x = \lambda_2 m^+{}_y = 0.232 m^+{}_y$$

$$m^-{}_y = \lambda_3 m^+{}_y = 0.20 m^+{}_y$$

According to EN-1992-2, the spacing of bars should not exceed $s_{max,slabs}$.

The recommended value is:
- for the principal reinforcement, $3h \leq 400$ mm, where h is the total depth of the slab;

- for the secondary reinforcement, $3.5h \leq 450$ mm.

In areas with concentrated loads or areas of maximum moment those provisions become respectively:

- for the principal reinforcement, $2h \leq 250$ mm

- for the secondary reinforcement, $3h \leq 400$ mm.

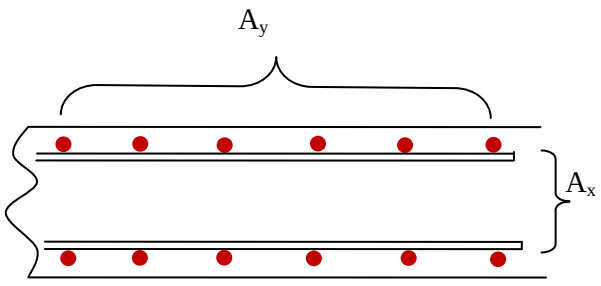

Φ16mm at s=75mm c/c

Chapter 4

ANALYSIS AND DESIGN OF SLAB USING YIELD LINE THEORY

4.1 Introduction

Yield line analysis is an analysis approach for determining the ultimate load capacity of reinforced concrete slabs and was pioneered by K.W. Johansen in the 1940s. It is closely related to the plastic collapse or limit analysis of steel frames, and is an Upper Bound or kinematical approach.

The ultimate load of the slab is estimated by postulating a collapse mechanism that is compatible with the boundary conditions. The moments at the plastic hinges are the ultimate moments of resistance of the section, and the ultimate load is determined using *the principle of virtual work*, or the *equations of equilibrium*. Being an upper-bound approach, the method gives an ultimate load for a given slab that is either correct or larger than the "true" value.

The Yield-line Method is only applicable to ductile (under-reinforced) slabs since we assume that the moment-rotation diagram given in Fig.9 holds.

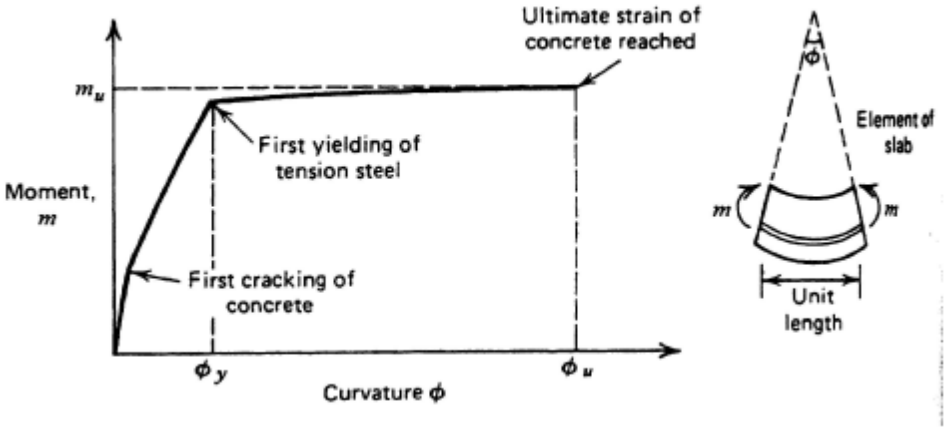

Fig:9 Moment-curvature relationship for a reinforced concrete slab section

4.2 Principles For Rigid-Plastic materials

As long as the stresses in a body of rigid-plastic material are below the yield point, no deformations occur. This idealization implies that we cannot determine the stress field in such a body when the stresses are below the yield point. When the loads increase to a point where it can be carried only by stresses at the yield points, unlimited deformations are possible without changing the loads. The body is then said to be subject to *collapse by yielding***.** The corresponding load is called *the collapse load* or *load carrying capacity* of the body.

Note that:

- a yield line occurs when the moment capacity of the section has been reached;
- no additional moments can be taken at the section;
- the section can undergo any amount of rotation.

4.3 Principle of Virtual work

Suppose that a rigid body is in equilibrium under the action of a system of forces. If the body is given a small arbitrary displacement, the sum of the work done by the forces(loads and internal forces) each force times its corresponding displacement will be zero because the resulting force is zero. Hence the principle of virtual work may be stated as:

"If a rigid body that is in statical equilibrium under a system of forces and reactions is given a virtual displacement, the sum of the virtual work done by the forces and reactions is zero."

To analyze the slab by the virtual-work method, a yield line pattern is postulated for the slab at the ultimate limit load. The segments of the yield line pattern may be regarded as rigid bodies because the slab deformation occurs only at the yield lines. The segments of the slabs are in equilibrium under the external loads and the bending and the shearing forces transferred along the yield lines.(twisting moments are disregarded in the classical Yield-line Method).

A convenient point within the slab is chosen and given a small displacement δ in the direction of the load. Then the resulting displacements at all the points of the slab, $\delta(x,y)$, and the rotations of the slab segments about the yield lines, may be found in terms of δ and the dimensions of the slab segments. Work will be done by external loads and by the internal forces along the yield lines.

The work done by a uniformly-distributed ultimate load per unit area w_u is

$$\iint w_u \, \delta(x,y) dx \, dy = \sum W_u \Delta \text{.....(Eq.8)}$$

Where:

- ✓ W_u is the total load on the segment of the yield line pattern.
- ✓ Δ is the down ward movements of its centroid.

The reactions at the supports will not contribute to the work, as they do not undergo any displacements.

The work done by the internal forces along the yield lines will be due only to the bending moments, because the work done by the twisting moments and by the shear forces is zero when summed over the whole slab, as these actions on each side of the yield lines are equal and opposite and for any displacement of the yield line pattern there is no relative movement between the sides of the yield line corresponding to the twisting moments and shear forces. However, there is a relative movement corresponding to the bending moments, since there is a relative rotation between the two sides of the yield line. Thus, the work done at the yield lines is due only to the ultimate (bending) moments.

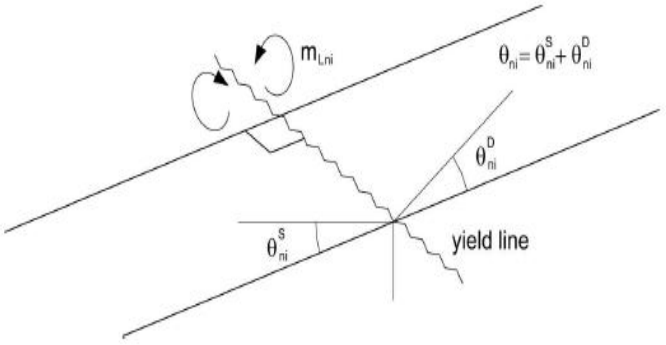

Fig:10 Action along the yield line (bending moment)

The work done by the ultimate moments of resistance per unit width m_{un} along a yield line of length l_o, where there relative rotation of the two segments around the yield line is θ_n is :

$$-m_{un}\theta_n l_o \ldots\ldots\ldots\ldots\ldots\ldots \text{(Eq.9)}$$

The work done here is negative because the bending moments will be acting in the direction opposite to the rotation if the slab is given a displacement in the direction of the load.

The total work done by the ultimate moments of resistance is obtained by summing the work done along all the yield lines:

$$\sum -m_{un}\theta_n l_o$$

Therefore, the virtual work equation may be written as:

$$0 = \sum W_u \Delta + \sum -m_{un}\theta_n l_o$$

or

$$\sum W_u \Delta = \sum m_{un}\theta_n l_o$$

When applied to a particular slab, the displacement terms cancels from the equation and the ultimate load is given in terms of the slab dimensions and the ultimate moments of resistance per unit width.

4.4 YIELD LINES

A slab is assumed to collapse at its ultimate load through a system of straight lines which are called *yield lines* (curved yield lines form only where required by the curved boundary, or when ever required by axis-symmetry).These yield lines divide the slab into a number of segments and this pattern of yield lines and segments is termed *the collapse mechanism*; a typical collapse mechanism for a simply supported rectangular slab carrying a uniformly-distributed load is shown in Fig. 11(a). The segments formed by the supports and by the yield lines are assumed to be plane (at fracture elastic deformations are small compared with plastic deformations and are ignored) and therefore must possess a geometric compatibility.

It is further assumed that the bending moment along all yield lines is constant and equal to the value corresponding to the yielding of the steel reinforcement. Also, the panels rotate about axes along the supported edges and, in a slab supported on columns, the axes of rotation pass through the columns, see Fig. 11(b). Finally, the yield lines on the sides of two adjacent panels pass through the point of intersection of their physical axes of rotation. Examples of yield line patterns are shown in Fig.12. Note the conventions for the representation of different support conditions.

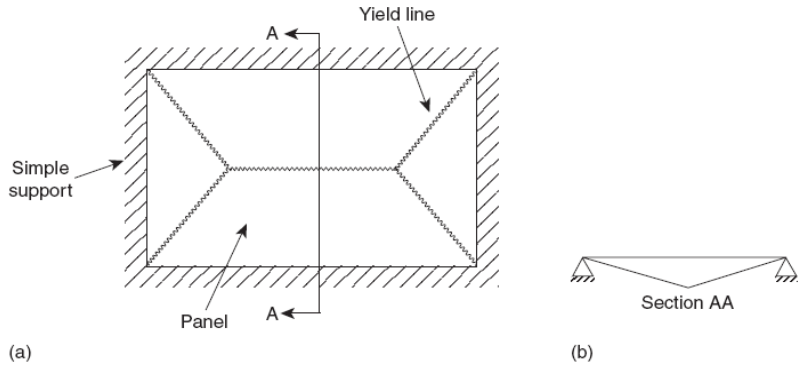

Fig. 11 Collapse mechanism for a rectangular simply supported slab

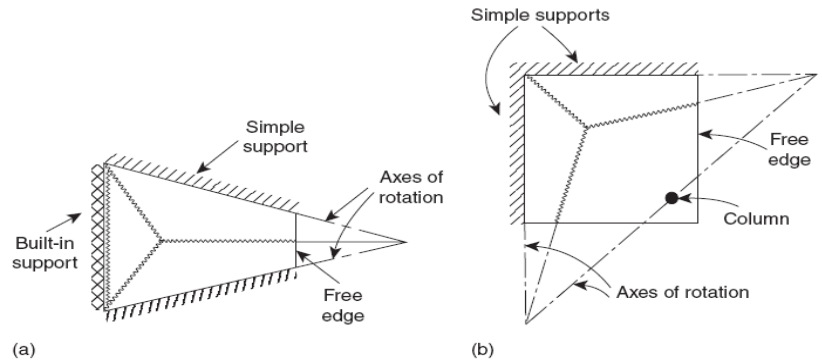

Fig 12. Collapse mechanisms and diagrammatic representation of support conditions.

4.4.1 Procedures for yield line analysis

- Assume a collapse mechanism by choosing a pattern of yield lines;
- Calculate the collapse load corresponding to that yield line pattern;
- Repeat for a range of yield line patterns;
- Actual failure occurs at the lowest collapse load.

Note that the use of the yield-line method, requires the slab to have the moment-rotation relationship previously given in the Fig. 9: sections must be ductile!

4.4.2 Conventions

- Sagging yield lines are represented as solid straight lines;
- Hogging yield lines are represented as dashed straight lines;
- A fixed support is indicated by double hatching;
- A simple support is given by single line hatching;
- A free edge is given by a straight line.

4.4.3 Rules for Yield Lines:

There are rules to be observed when postulating a yield line pattern:

- Yield lines divide the slab into rigid regions (segments) which remain plane through the collapse;
- Yield lines are straight;
- Axes of rotation generally lie along lines of support and pass over any columns;
- Yield lines between adjacent rigid regions must pass through the point of intersection of the physical axes of rotation of those regions;
- Yield lines must end at a slab boundary;
- Continuous supports repel and simple supports attract yield lines.

4.5 ULTIMATE MOMENT ALONG A YIELD LINE

Johansen's Stepped Yield Line Criterion

This is the basic assumption of yield line theory. It assumes that during the rotation the bars remain in their original direction and do not 'kink'. It is also valid for slabs that are not of reinforced concrete. Johansen's Stepped yield line criterion says that the yield line is actually made up of many small steps in orthogonal directions, as shown in Fig.13a. below.

This, in turn, enables us to take the *projections of an inclined yield line upon the axes*, instead of determining the capacity at an angle.

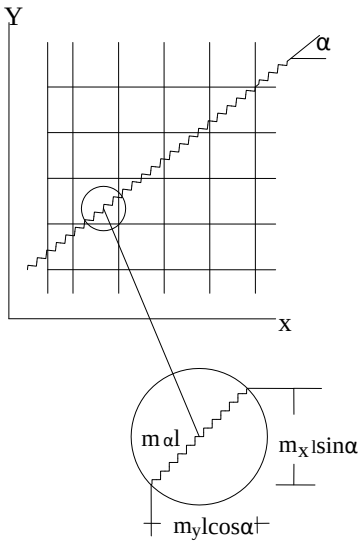

Fig 13a. Determination of the Ultimate moment along the yield line.

Figure 13a, shows a portion of a slab reinforced in two directions at right angles; the ultimate moments of resistance of the reinforcement are m_x and m_y per unit width of slab in the y and x directions, respectively. Let us suppose that a yield line occurs at an angle α to the reinforcement in the x-direction

Now consider a triangular element formed by a length *l* of the yield line and the reinforcement as shown in Fig. 13b below.

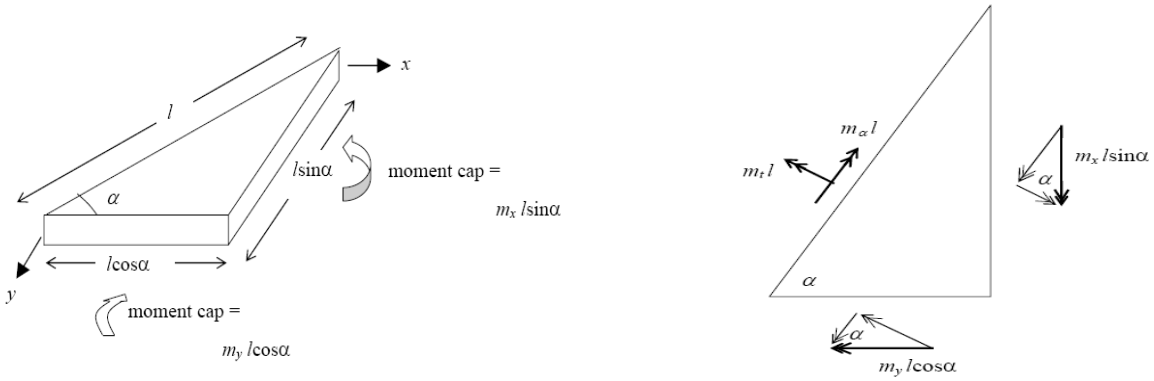

Figure: 13b. triangular element for ultimate moment along the yield line

Then, from the moment equilibrium of the element in the direction of m_α, we have

$$m_\alpha . l = m_x . lsin^2\alpha + m_y . lcos^2\alpha$$

$$m_\alpha = m_x sin^2\alpha + m_y cos^2 \ldots\ldots\ldots\ldots \text{(Eq.10)}$$

Using all the above explanations and assumptions, we can start to apply them to our slab.

4.6 Ultimate load calculation at room temperature using yield lines.

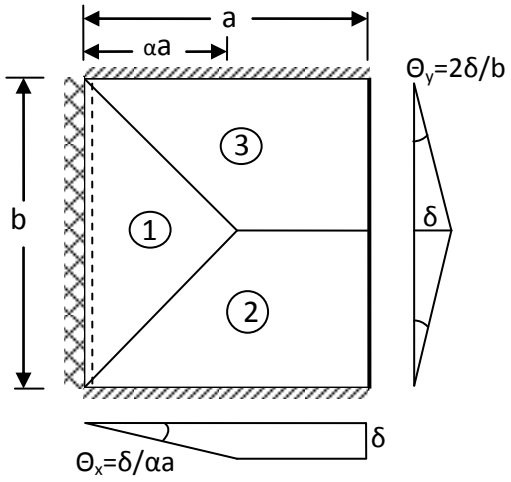

Case 1

External work done due to distributed load $p(\frac{KN}{m^2})$

$$W_E{}^1 = \frac{p\left(\frac{1}{2}\alpha.a.b\right)\delta}{3} = p(\alpha.a.b)\frac{\delta}{6}$$

$$W_E{}^2 = W_E{}^3 = \frac{p\left(\frac{1}{2}\alpha.a.\frac{b}{2}\right)\delta}{3} + p(1-\alpha).a.\frac{b}{2}.\frac{\delta}{2}$$

$$W_E{}^{tot} = W_E{}^1 + W_E{}^2 + W_E{}^3$$

$$W_E{}^{tot} = p\left[\alpha.a.b.\frac{\delta}{3} + (1-\alpha).a.b.\frac{\delta}{2}\right]$$

Internal work done:

Sagging moment: $W_i{}^1 = m^-{}_x.b.\theta_x = \lambda_2 m^+{}_y.b.\theta_x$

Hogging moment: $W_i{}^{1,2,3} = m^+{}_x.b.\theta_x + 2m^+{}_y.a.\theta_y = \lambda_1 m^+{}_y.b.\theta_x + 2m^+{}_y.a.\theta_y$

$$W_i{}^{tot} = m^-{}_x.b.\theta_x + m^+{}_x.b.\theta_x + 2m^+{}_y.a.\theta_y$$

$$= m^-{}_x.b.\frac{\delta}{\alpha.a} + m^+{}_x.b.\frac{\delta}{\alpha.a} + 2m^+{}_y.a.\frac{2\delta}{b}$$

$$W_i{}^{tot} = m^+{}_y\left[(\lambda_1+\lambda_2).\frac{b}{a}.\frac{\delta}{\alpha} + 4\frac{a}{b}.\delta\right]$$

Equating the external and internal work equations above:

$$p_{u,1} = \frac{m^{+}{}_{y}\left[(\lambda_1 + \lambda_2).\frac{b}{a}.\frac{\delta}{\alpha} + 4\frac{a}{b}.\delta\right]}{\left[\alpha.a.b.\frac{\delta}{3} + (1-\alpha).a.b.\frac{\delta}{2}\right]}$$

$$p_{u,1} = \frac{m^{+}{}_{y}\left[(\lambda_1 + \lambda_2).\frac{b}{\alpha a}.+4\frac{a}{b}\right]}{\left[\alpha.a.\frac{b}{3} + (1-\alpha).a.\frac{b}{2}\right]} \ldots\ldots\ldots\ldots\ldots\ldots\ldots\ldots..(Eq.11)$$

The maximum value of $p_{u,1}$ with respect to a changing α occurs at: $\frac{dp_{u,1}}{d\alpha} = \mathbf{0}$

Let $k = 6m^{+}{}_{y}\left[(\lambda_1 + \lambda_2).\frac{b}{a}\right]$

$L = 24m^{+}{}_{y}\frac{a}{b}$ and $n = a.b$

Thus, $P_{u,1}$ can be simlified as: $p_{u,1} = \frac{\frac{K}{\alpha}+L}{3n-n\alpha}$;

$$\frac{dp_{u,1}}{d\alpha} = \frac{\frac{-K}{\alpha^2}(3n-n\alpha)+n(\frac{K}{\alpha}+L)}{(3n-n\alpha)^2} = \mathbf{0}$$

$$\alpha^2 L + 2\alpha K - 3K = 0$$

This is a quadratic equation in terms of $\boldsymbol{\alpha}$:solve to get:

$$\alpha = \frac{K}{L}(-1 + \sqrt{(1 + \frac{3L}{K})}$$

Substituting all the variables:

$$\alpha = \frac{(\lambda_1+\lambda_2)\frac{b^2}{a^2}}{4}\left[-1 + \sqrt{1 + \frac{12\frac{a^2}{b^2}}{(\lambda_1+\lambda_2)}}\right] \rightarrow\rightarrow\rightarrow \boldsymbol{\alpha = 0.534} \qquad (\mathbf{0} < \alpha \leq 1) \ldots\ldots\ldots\ldots\ldots\ldots\text{(Eq. 12)}$$

It is for this value of $\boldsymbol{\alpha}$ that the slab will fail, given the dimensional and strength data.

$$p_{u,1} = \frac{6m^{+}{}_{y}\left[(\lambda_1 + \lambda_2).\frac{b}{\alpha a}.+4\frac{a}{b}\right]}{a.b(3-\alpha)} = 25.313\frac{kN}{m^2}$$

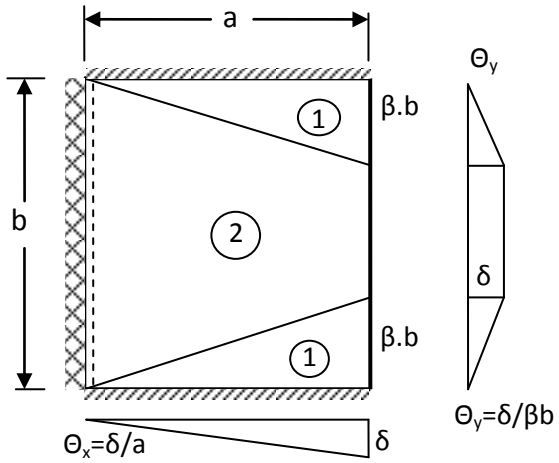

Case 2

External Work Done due to distributed load $p(\frac{KN}{m^2})$

$$W_E{}^1 = \frac{p.2\left(\frac{1}{2}\beta.b.a\right)\delta}{3} = p.(\beta.b.a)\frac{\delta}{3}$$

$$W_E{}^2 = p.2\left(\tfrac{1}{2}\beta.b.a\right)\delta + (a.b(1-2\beta)\tfrac{\delta}{2}$$

$$W_E{}^{tot} = p\left[\tfrac{2\beta}{3}(a.b)\delta + a.b(1-2\beta)\tfrac{\delta}{2}\right]$$

Internal Work Done:

Sagging moment: $W_i{}^1 = m^-{}_x.b.\theta_x = \lambda_2 m^+{}_y.b.\theta_x$

Hogging moment: $W_i{}^{1,2} = 2m^+{}_x.\beta b.\theta_x + 2m^+{}_y.a.\theta_y = 2\lambda_1 m^+{}_y.\beta b.\theta_x + 2m^+{}_y.a.\theta_y$

$$W_i{}^{tot} = m^-{}_x.b.\theta_x + 2m^+{}_x.\beta b.\theta_x + 2m^+{}_y.a.\theta_y$$

$$= m^-{}_x.b.\frac{\delta}{a} + 2m^+{}_x.\beta b.\frac{\delta}{a} + 2m^+{}_y.\frac{\delta.a}{\beta b}$$

$$W_i{}^{tot} = 2m^+{}_y.\delta(\frac{a}{\beta b} + \lambda_1\frac{\beta b}{a} + \lambda_2\frac{b}{2a})$$

Equating the external and internal work equations above:

$$p_{u,2} = \frac{2m^+{}_y(\frac{a}{\beta b} + \lambda_1\frac{\beta b}{a} + \lambda_2\frac{b}{2a})}{\left[\frac{2\beta}{3}(a.b) + a.\frac{b}{2}(1-2\beta)\right]}$$

$$p_{u,2} = \frac{12m^{+}{}_{y}(\frac{a}{\beta b}+\lambda_1\frac{\beta b}{a}+\lambda_2\frac{b}{2a})}{a.b(3-2\beta)}$$ …… (Eq. 13)

The maximum value of $p_{u,2}$ with respect to a changing β occurs at: $\frac{dp_{u,2}}{d\beta} = \mathbf{0}$

Let $R = 12m^{+}{}_{y}\frac{a}{b}$

$$H = 12m^{+}{}_{y}.\lambda_1\frac{b}{a}$$

$$T = 12m^{+}{}_{y}.\lambda_2\frac{b}{2a}$$

Thus, $p_{u,1}$ can be simlified as: $p_{u,2} = \frac{\frac{R}{\beta}+\beta H+T}{3n-n\beta}$;

$$\frac{dp_{u,2}}{d\beta} = \beta^2(3H+2T)+4\beta R-3R = 0$$

Substituting all the variables:

$$\beta = \frac{-2+\sqrt{4+3(3\lambda_1+\lambda_2)\frac{b^2}{a^2}}}{(3\lambda_1+\lambda_2)\frac{b^2}{a^2}} \rightarrow\rightarrow\rightarrow \boldsymbol{\beta = 0.649} \qquad \mathbf{0} < \beta \leq 0.5$$……(Eq. 14)

$$P_{u,2} = \frac{12m^{+}{}_{y}(\frac{a}{\beta b}+\lambda_1\frac{\beta b}{a}+\lambda_2\frac{b}{2a})}{a.b(3-2\beta)}$$

As it is shown above the value of $\boldsymbol{\beta}$ does not comply with the limitation. From this we can conclude that the two cases are said to be "*mutually incompatible*", which means that , if one case satisfies the limitation, the other case does not satisfy the limitation; hence the first is the only one " kinematically consistent".

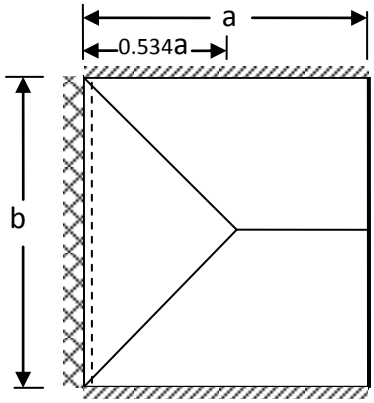

Figure:14 Yield-line pattern for case 1. (α=0.534a)

Chapter 5

FIRE CALCULATION OF THE SLAB

5.1 Introduction

Fires are caused by accident, energy sources or natural means, but the majority of fires in buildings are caused by human errors. Once a fire starts and the contents and/or materials in a compartment are burning, then the fire spreads via radiation, convection or conduction with flames reaching temperatures between 600°C and 1200°C. Harm is caused by a combination of the effects of smoke and gases, which are emitted from burning materials, and the effects of flames and high air temperatures.

The behaviour of a structure exposed to fire is usually described in terms of fire resistance, which is the period of time required the structure to reach a limit situation when exposed to a fire (standard fire or natural fire), generally represented by means of a temperature-time curve. In performance-based design this limit situation may be defined as *structural collapse* or *loss of integrity* (which allows the fire-spread to occur), but is more usually defined in terms of deflection. Current design codes have taken a step towards full performance-based design by allowing designers to treat fire as one of the basic design limit states, taking account of:

- The level of loading in fire, using partial safety factors lower than those used in ultimate limit states, because of very small likelihood to have a fire under ultimate loads.
- The fire load, represented by the actual quantities of the combustible material expressed in terms of heat or heat rate (thermal power) per square meter.
- Non-uniform heating due to partial protection, which may be inherent in the framing systems or may be on purpose applied.
- Realistic stress-strain characteristics of the materials at elevated temperatures.

5.2 CONCRETE IN FIRE.

Concrete does not burn – it cannot be 'set on fire' like other materials (as timber or plastics) in a building and it does not emit any toxic fumes when affected by fire. It will produce no smoke or drip molten particles, unlike some plastics and metals; hence it does not add to the fire load. For these reasons concrete is said to have a high degree of fire resistance and in most applications, concrete can be described as virtually 'fireproof'.

This excellent performance is due mostly to concrete's constituent materials (i.e. cement, aggregates and water) which, when chemically combined within concrete, form a material that is essentially inert and has a rather poor thermal conductivity, something that is a plus in fire safety. It is this slow rate of heat transfer (conductivity) that enables concrete to act as an effective fire shield not only between adjacent spaces, but also to protect itself from fire damage. The rate of increase of temperature through the cross section of a concrete member is rather slow and so the internal zones do not reach the high temperatures reached by the surface exposed to flames.

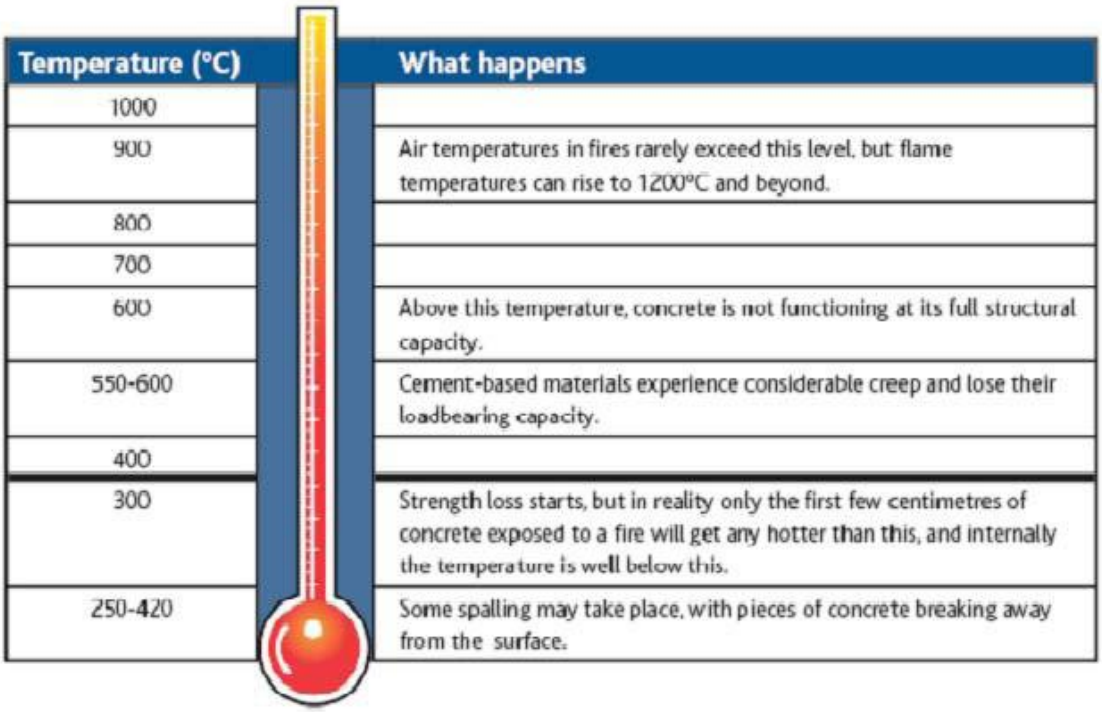

Temperature (°C)	What happens
1000	
900	Air temperatures in fires rarely exceed this level, but flame temperatures can rise to 1200°C and beyond.
800	
700	
600	Above this temperature, concrete is not functioning at its full structural capacity.
550-600	Cement-based materials experience considerable creep and lose their loadbearing capacity.
400	
300	Strength loss starts, but in reality only the first few centimetres of concrete exposed to a fire will get any hotter than this, and internally the temperature is well below this.
250-420	Some spalling may take place, with pieces of concrete breaking away from the surface.

Fig:15 Concrete in fire –chemo-physical processes.

5.3 Numerical Model

In fire modelling, the heating of a concrete slab is represented as a one-dimensional heat-transfer problem. For one-dimensional heat transfer by conduction in a material with no internal heat being released, the governing equation is as follows (see for instance by Buchanan,2001)

$$\frac{\delta^2 T}{\delta x^2} = \frac{1}{\alpha}\frac{\delta T}{\delta t} \quad \text{..... (Eq. 14)}$$

where: t is the time (s), T is the temperature (°C or K), x is the distance in the direction of heat flow and α is the thermal diffusivity (m^2/s)

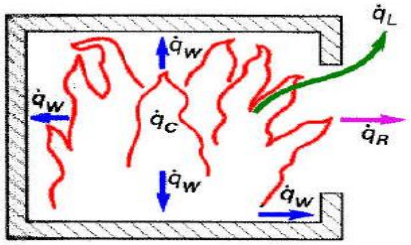

Fig:16 Heat balance for a post-flashover (i.e fully developed) room fire.

Starting from the previous equation and using numerical tools, the temperatures across the cross section of a slab can be calculated. For the calculation of these temperatures, only the properties of concrete are considered and the reinforcement is assumed to have no influence on the thermal field. This can be justified on the basis of the smallness of that the reinforcement cross section compared to the concrete section. However, once the thermal field is known, the reinforcement can be given the same temperatures of the surrounding concrete and in this way the mechanical decay of the reinforcement can be taken care of.

5.4 Time-temperature Curves

The time-temperature curves used in fire resistance tests are called the "standard fires". As shown in the figure 17 below, the most widely used test specifications are ASTM E119 and the ISO 834. All other international fire resistance test standards specify similar time-temperature curves(Lie, 1995).

Fire Tests

Fire tests represent the oldest method to evaluate the fire endurance of structural elements. As early as 1918, fire tests were being performed on building columns at the Laboratories (1918). Fire tests expose structural elements to different fire severities and are either performed within a furnace or on full-scale buildings. Many countries use full-scale fire resistance tests to evaluate the fire performance of structural elements. Full-scale tests are preferred for the study of structural elements and assemblies of a relatively small extent because they give a more accurate representation of the various phenomena that occur during fire conditions such as the effects of thermal expansion and deformation under load

Furnace Testing

Test furnaces are the most common method used to evaluate the fire resistance of structural elements. The furnaces' chamber is heated either electronically or by burning liquid fuel. The temperature history in the furnace is controlled by a designated fire curve, typically those of "standard fires". Usually, furnaces are equipped with devices to measure temperatures, and deformations, and to load test specimens. Furnaces follow different testing specifications depending on the laboratory and are specially constructed for their purpose. There are vertical furnaces that are constructed for testing vertical partitions such as walls and doors; horizontal furnaces are used for testing horizontal partitions such as floors and roofs. Also, there are special beam and columns furnaces, although they are often tested in horizontal furnaces. Some furnaces are even designed so that all types of building elements can be tested.

Fire tests in furnaces are carried out by exposing certain surfaces of a test specimen to heating in a manner that simulates its exposure to heating in a fire (Abrams & Gustaferro 1968; Wade 1992). Generally, test specimens are construction elements for which a fire resistance classification is desired. Specimens are tested under conditions that are similar to those in service such as loading and restraint. Thermocouples are placed in the furnace and within specimens to measure temperatures. A specimen is considered fire resistant during a test up until the point it does not satisfy certain testing criteria with respect to stability, integrity, and thermal insulation.

Full-Scale Fire Tests

Occasionally full-scale fire tests are performed on structural systems. These tests give a more realistic representation of fire performance because they simulate the performance of a system as opposed to the study of discrete elements or small-scale assemblies. The major drawback of full-scale testing is that it is extremely expensive in comparison with furnace testing. The most comprehensive full-scale testing completed took place in 1995 in Cardington, England. A series of fire tests were carried out on an eight-storey, steel-concrete composite structure. As an outgrowth of the Cardington tests, numerous numerical and theoretical models have been developed to simulate the performance of the structure. The test results and the subsequent models have deepened understanding of the mechanical behavior of highly redundant structures in extreme fires.

Standard Fires

Most fire resistance tests follow time-temperature curves that serve as “standard fires” which are idealized simulations of room fires. Since the tests follow established time-temperature curves, the heat load imposed on a test specimen is calculable at any point during testing. Standard fire test time-temperature curves for various countries shows slight difference (Lie 1995). The most widely used standard test conditions are the ASTM E119 (United States and Canada) and ISO 834 (Australia, New Zealand, and England) (Buchanan 2001)

In the ISO 834 specification (ISO 1975) the temperature T(°c) is defined by

$$T = 345log10^{(8t+1)} + T_0$$

Where t is the time (minutes) and T_0 is the ambient temperature (°C)

The ASTM E119 curve is defined by a number of discrete points. Several equations approximating the ASTM E119 curves are given by Lie (1995), the simplest of which gives the temperature T(°C) as:

$$T = 750\left[1 - e^{-3.79553\sqrt{t_h}}\right] + 170.41\sqrt{t_h} + T_0$$

In the figure it is also shown the hydrocarbon fire curve. The temperature for the hydrocarbon fire curve is given by

$$T = 1080(1 - o.325e^{-0.167t} - 0.675e^{-2.5t}) + T_0$$

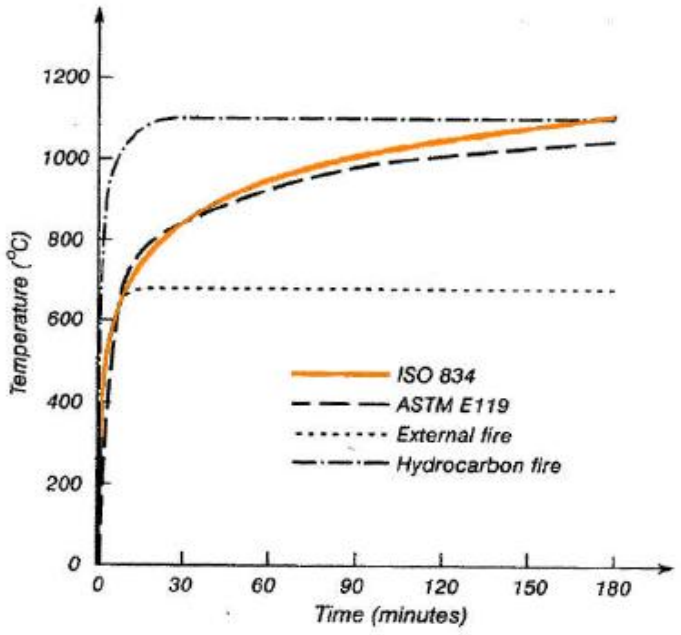

Fig:17 standard time-temperature curve

5.5 Materials Properties

In the analysis, only the thermal properties of concrete, *density*, *thermal conductivity* and *specific heat*, as a function of the temperature, are required. These properties are built into the program(ABAQUS). The mechanical properties, such as the stress-strain relationship, are not required since only a thermal analysis is carried out; however, the critical temperature for the reinforcement, at which the strength degradation reaches a specific value, has to be specified.

5.5.1 Density of concrete

The ***density*** of concrete depends on the aggregate and the mix design. Typical dense concrete has a density of about 2300kg/m^3. There are many 'lightweight' concretes which use porous aggregates or air entrainment to reduce the density. When heated to 100°C the density of most concretes will be reduced by up to100kg/m^3 due to the evaporation of free water. Other than moisture changes, the density of the concrete doesn't change much at elevated temperature, except for limestone(calcareous) aggregate concrete which decomposes above 800°C.

$\rho(t) = \rho(20℃)$ for $20℃ \le t \le 115℃$

$\rho(t) = \rho(20℃) \cdot (1 - 0.02\,(t - 115) / 85)$ for $115℃ < t \le 200℃$

$\rho(t) = \rho(20℃) \cdot (0.98 - 0.03\,(t - 200) / 200)$ for $200℃ < t \le 400℃$

$\rho(t) = \rho(20℃) \cdot (0.95 - 0.07\,(t - 400) / 800)$ for $400℃ < t \le 1200℃$

EC-2 part 1-2 (2004)

density of concrete	
ρ(kg/m^3)	T(°C)
2400	20
2400	115
2352	200
2280	400
2112	1200

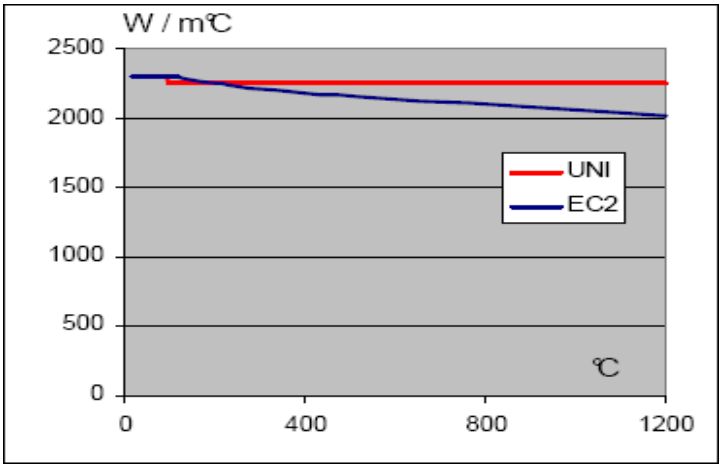

Figure:18 density of concrete at elevated temperature

5.5.2 Thermal Conductivity and specific heat.

The ***thermal conductivity*** of concrete is temperature dependent, and varies depending on the type of aggregate. Approximate values for design purpose are 1.6W/mK for siliceous concrete and 1.3W/mK for calcareous(limestone) aggregate concrete, and 0.8W/mK for light weight concrete. (EC2).

Thermal conductivity	
λ(W/mK)	T(°C)
1.68	0
1.5	100
1.33	200
1.18	300
1.05	400
0.93	500
0.83	600
0.75	700
0.68	800
0.63	900
0.59	1000
0.58	1100
0.57	1200

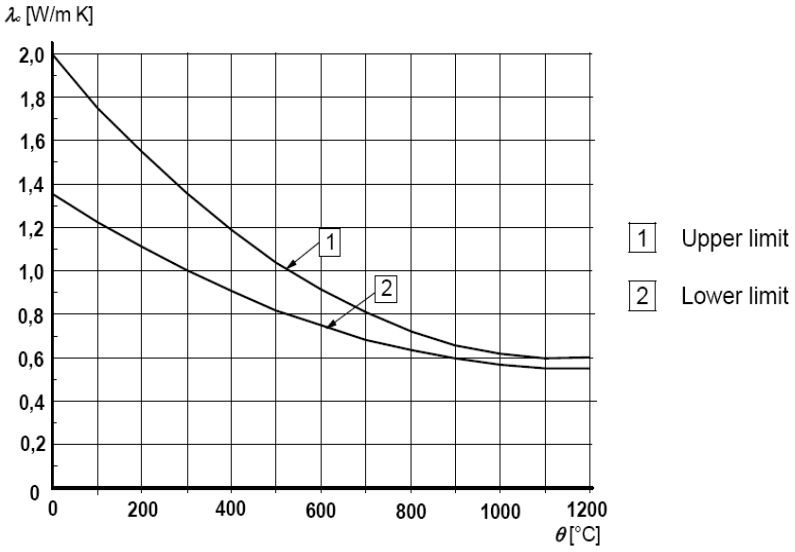

Fig:19 Thermal conductivity of concrete

The specific heat of concrete also varies depending on the moisture content, with design values from EC2 (2004) for three different moisture content is shown in the figure 20 below. The peak between 100 and 200°C allows for the water being driven off during the heating process.

Specific heat	
Cp(θ)	T(°C)
900	20
900	100
1000	200
1100	400
1100	1200

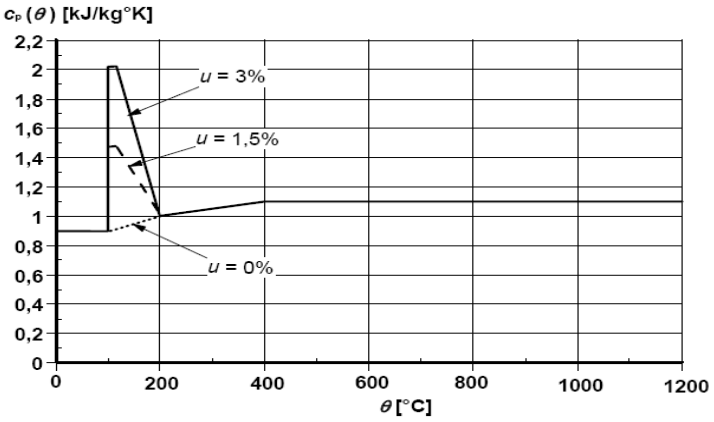

Figure:20 specific heat of concrete

Essentially, the temperatures at the location of the reinforcing steel and at various concrete depths can be approximated using the temperature distribution charts for different values of the fire duration. Once the temperatures are known, relationships for the mechanical properties at high temperature can be used (Tables 3 & 4 and graphs 21 & 24 below), in conjunction with the usual equations used for moment resistance calculations to approximate the nominal moment capacities of steel-reinforced slabs in either positive or negative bending.

Fire design of reinforced-concrete flexural members is often accomplished by assuming that structural failure under service loads will occur when the principal tensile reinforcement reaches a temperature of 593°c. This approach is rational, defensible, and conservative when using steel reinforcement. It is important to recognize, however, that the choice of the critical temperature for steel arises as a consequence of the assumed failure mode of the steel-reinforced members.

The result is that a temperature of 593°c in the reinforcing steel corresponds to about a 50% reduction in the yield strength of the reinforcement, which in turn corresponds to about a 50% reduction in the flexural capacity of the section; and finally, which corresponds roughly to structural collapse under the unfactored service loads.

It is worth noting that two-way reinforcement, continuity, and lateral restraint are also known to be important factors in the structural fire performance of concrete slabs . However, continuity and lateral restraint typically tend to improve the fire performance of well-designed steel-reinforced concrete slabs.

Thus, the following discussion and calculation focuses on the behavior of simply-supported slabs that are unrestrained against changes in axial length. In most cases this is a conservative treatment with respect to structural fire resistance.

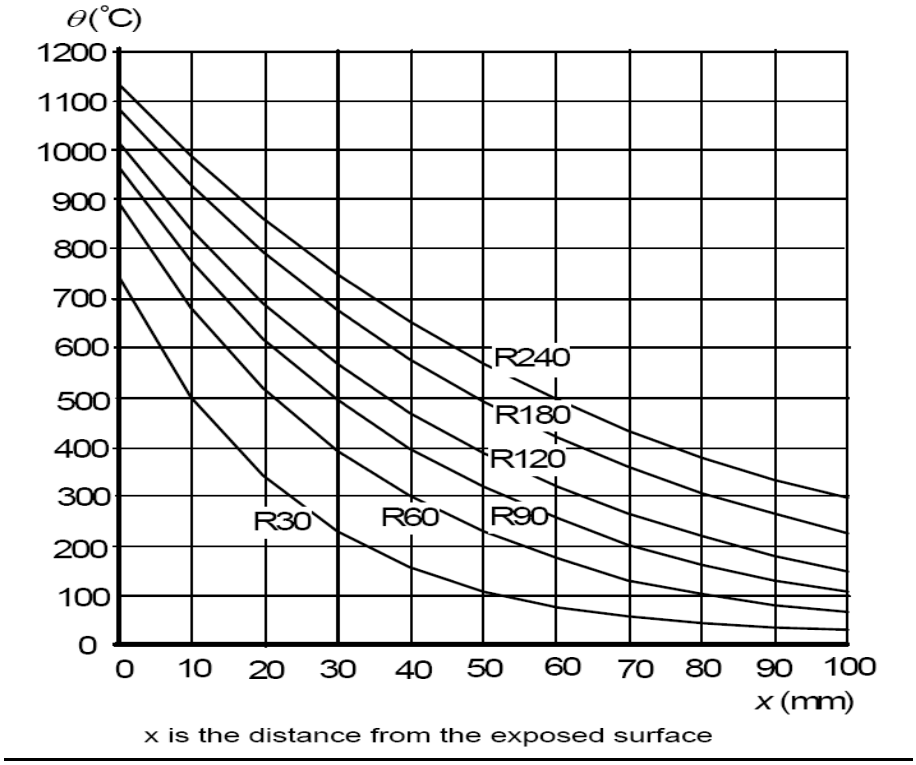

Figure:21 Temperature across the slab

5.6 Flexural strength analysis

Once the distribution of temperatures throughout the slab is known at any instant in time, an approximation of the slab's flexural capacity can be obtained using a simple incremental plane-sections analysis. The following assumptions are required for the analysis:

1. Concrete has no strength in tension.
2. Plane-sections before bending remain plane after bending.
3. There is perfect bond between the reinforcement and the concrete.
4. The thermo-mechanical properties of concrete, reinforcing steel, are described by the mathematical relationships presented in the codes.
5. The slab is unrestrained against expansion in the lateral direction.
6. Fire exposure is from below.

Reduced section method (500°C isotherm)

This method was first proposed by Anderberg (1978), following the analysis of fire tests carried out on flexural reinforced concrete elements. There are some limitations placed on the method and comprise minimum thicknesses for either standard exposure times or fire load densities.(Table B1: EN 1992-1-2)

The calculations are carried out by assuming:

1. The concrete within the 500°C isotherm remains unaffected by heat.
2. The reduction factors for the reinforcement (assuming class N) are for:
    - Compression and tension reinforcement with the strain in the ε_{fi}>2%.

Using the above assumptions and the known distribution of temperatures in the concrete at any time during fire exposure (obtained from the heat transfer analysis), the flexural capacity of the slab can be approximated, in this case for an assumed 1 m wide strip of the cross-section, using a traditional force-equilibrium approach.

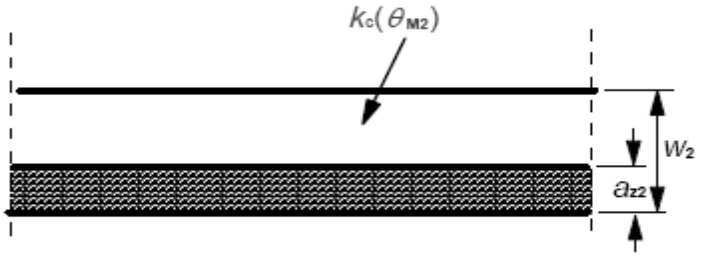

Figure: 22 Cross section of the slab damaged during fire

For each fire duration the neutral axis depth in all the sections is found, exploiting the equilibrium to the translation:

$$y^T = \frac{f^T{}_{yk}.A_s}{0.85.b.f_{ck}} \quad \text{.....(Eq. 15)}$$

Effective depth

- For the bar layers closest to the concrete surface (y-direction)

$$d' = h - c - \frac{\emptyset}{2} = 300 - 30 = 270mm$$

- For the bar layers farthest from concrete surface (x-direction)

$$d'' = h - c - \emptyset - \frac{\emptyset}{2} = 300 - 30 - 16 = 254mm$$

In this way the internal arm $z^T = d - \frac{y^T}{2}$ is obtained, and then we can evaluate the new resisting moments for each fire condition:

$$m_{rd}{}^{T} = A_s . f_{yk}{}^{T} . Z^{T} \text{.....(Eq. 16)}$$

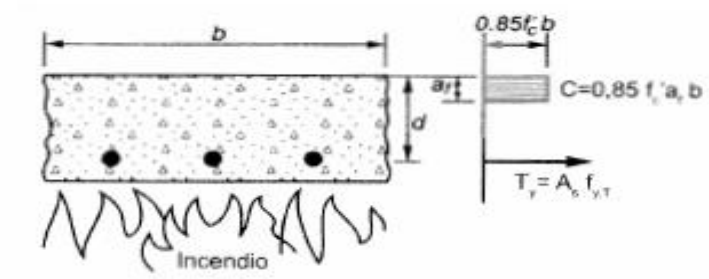

In any sections subjected to negative bending, the effective depth and the internal lever arm decreases because of the damage in the compressed concrete exposed to the fire. For instance, the concrete above 500°C should be neglected.

$$\alpha = \frac{(\lambda_1 + \lambda_2)\frac{b^2}{a^2}}{4}\left[-1 + \sqrt{1 + \frac{12\frac{a^2}{b^2}}{(\lambda_1 + \lambda_2)}}\right]$$

$$\beta = \frac{-2 + \sqrt{4 + 3(3\lambda_1 + \lambda_2)\frac{b^2}{a^2}}}{(3\lambda_1 + \lambda_2)\frac{b^2}{a^2}}$$

Finally, substituting the moment resistance in to the two cases of the yield line load carrying capacity equations, we can obtain the collapse load due fire condition.

$$P_{u,1} = \frac{6m^{+}{}_{y}\left[(\lambda_1+\lambda_2).\frac{b}{\alpha a}.+4\frac{a}{b}\right]}{a.b(3-\alpha)}$$

and

$$P_{u,2} = \frac{12m^{+}{}_{y}(\frac{a}{\beta b}+\lambda_1\frac{\beta b}{a}+\lambda_2\frac{b}{2a})}{a.b(3-2\beta)}$$

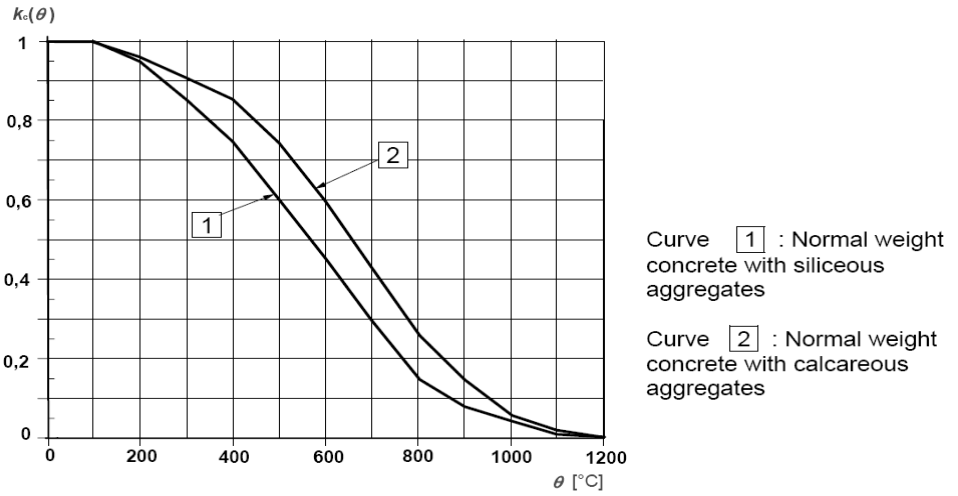

Figure: 23 Coefficient *k*c(θ) allowing for decrease of characteristic strength (*f*ck) of Concrete (EN-1992-1-2)

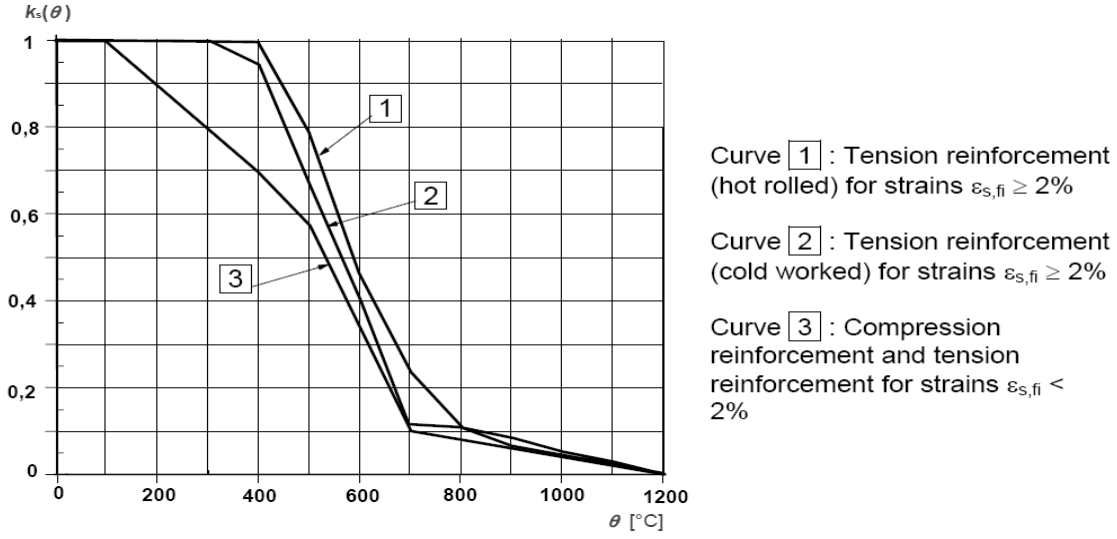

Figure:24 Coefficient *k*s(θ) allowing for decrease of characteristic strength (*f*yk) of tension and compression reinforcement (Class N)

Steel Temperature θ [°C]	$f_{sy,\theta} / f_{yk}$		$f_{sp,\theta} / f_{yk}$		$E_{s,\theta} / E_s$	
	hot rolled	cold worked	hot rolled	cold worked	hot rolled	cold worked
1	2	3	4	5	6	7
20	1,00	1,00	1,00	1,00	1,00	1,00
100	1,00	1,00	1,00	0,96	1,00	1,00
200	1,00	1,00	0,81	0,92	0,90	0,87
300	1,00	1,00	0,61	0,81	0,80	0,72
400	1,00	0,94	0,42	0,63	0,70	0,56
500	0,78	0,67	0,36	0,44	0,60	0,40
600	0,47	0,40	0,18	0,26	0,31	0,24
700	0,23	0,12	0,07	0,08	0,13	0,08
800	0,11	0,11	0,05	0,06	0,09	0,06
900	0,06	0,08	0,04	0,05	0,07	0,05
1000	0,04	0,05	0,02	0,03	0,04	0,03
1100	0,02	0,03	0,01	0,02	0,02	0,02
1200	0,00	0,00	0,00	0,00	0,00	0,00

Table:3 Class N values for the parameters of the stress-strain relationship of hot rolled and cold worked reinforcing steel at elevated temperatures.

Concrete temp. θ	Siliceous aggregates			Calcareous aggregates		
	$f_{c,\theta} / f_{ck}$	$\varepsilon_{c1,\theta}$	$\varepsilon_{cu1,\theta}$	$f_{c,\theta} / f_{ck}$	$\varepsilon_{c1,\theta}$	$\varepsilon_{cu1,\theta}$
[°C]	[-]	[-]	[-]	[-]	[-]	[-]
1	2	3	4	5	6	7
20	1,00	0,0025	0,0200	1,00	0,0025	0,0200
100	1,00	0,0040	0,0225	1,00	0,0040	0,0225
200	0,95	0,0055	0,0250	0,97	0,0055	0,0250
300	0,85	0,0070	0,0275	0,91	0,0070	0,0275
400	0,75	0,0100	0,0300	0,85	0,0100	0,0300
500	0,60	0,0150	0,0325	0,74	0,0150	0,0325
600	0,45	0,0250	0,0350	0,60	0,0250	0,0350
700	0,30	0,0250	0,0375	0,43	0,0250	0,0375
800	0,15	0,0250	0,0400	0,27	0,0250	0,0400
900	0,08	0,0250	0,0425	0,15	0,0250	0,0425
1000	0,04	0,0250	0,0450	0,06	0,0250	0,0450
1100	0,01	0,0250	0,0475	0,02	0,0250	0,0475
1200	0,00	-	-	0,00	-	-

Table:4 Values for the main parameters of the stress-strain relationships of normal weight concrete with siliceous or calcareous aggregates concrete at elevated temperatures**.**

For intermediate values of the temperature, linear interpolation should be used.

The strength and deformation properties of reinforcing steel at elevated temperatures shall

be obtained from the stress-strain relationships specified in EN-1992-1-2

Chapter 6

STANDARD FIRE CALCULATION FOR THE SLAB

The strength reduction of steel depends on the temperature, considering the bar cover. Seven fire durations are considered (from R30 to R300), and for each of them the corresponding temperature is evaluated with reference to Figure 21, with a bar cover equal to 30mm for y-direction bars and 46mm for x-direction bars. For each temperature the reduction factor ks(θ) of the characteristic yield strength comes from Figure 24. Corresponding temperatures and reduction factors for each condition are listed in Table below. Also the case at ambient temperature is considered (with characteristic strengths) to make a comparison with the fire conditions.

NOTE: Temperature profiles for standard fire resistance of slab sections given in the Annex A of EN 1992-1-2 (Figure 24) implies that these profiles are results of calculation. It is not, however, known whether these profiles are calibrated against actual test data.

Worked Example for fire duration (R90)

1. Effective depth

- For the bar layers closest to the concrete surface (y-direction)

$$d' = h - c = 300 - 30 = 270mm$$

- For the bar layers farthest from concrete surface (x-direction)

$$d'' = h - c - \emptyset - \frac{\emptyset}{2} = 300 - 30 - 16 = 254mm$$

2. Temperatures at the centroid of the reinforcements and corresponding reduction in strength from figure 24 and table

y-direction: T=495°C; ks(θ)=0.791

x-direction: T=360°C; ks(θ)=1.0

3. Neutral axis position

For each fire duration the neutral axis depth in all the sections is found, exploiting the equilibrium to the translation (Equation 15)

$$y^T = \frac{f^T{}_{yk}.A^{+y}{}_s}{0.85.b.f_{ck}} = \frac{(0.791 * 500 * 2998)}{0.85 * 30 * 1000} = 46.5mm\ from\ the\ top\ (+y\ reinforcement)$$

$$y^T = \frac{f^T{}_{yk}.A^{+x}{}_s}{0.85.b.f_{ck}} = \frac{(1.0 * 500 * 267)}{0.85 * 30 * 1000} = 10.48mm\ from\ the\ top\ (+x\ reinforcement)$$

$$y^T = \frac{f^T{}_{yk}.A^{+x}{}_s}{0.85.b.f_{ck}} = \frac{(1.0 * 500 * 644)}{0.85 * 30 * 1000} = 40.62mm\ from\ the\ bottom\ (-x\ reinforcement)$$

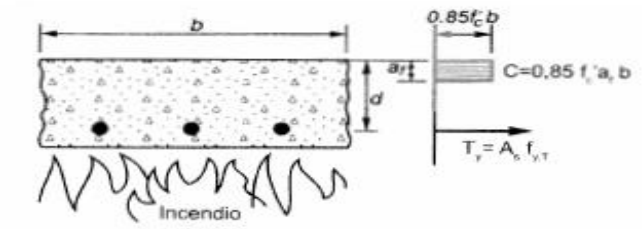

Note that, for the –ve reinforcement, y^T=12.62mm from the 500°C isotherm which is 28mm from bottom.

4. Internal lever arms

The internal arm is obtained using the equation, $z^T = d - \frac{y^T}{2}$

- For +y reinforcement $z^T = d' - \frac{y^T}{2} = 270 - \frac{46.5}{2} = 223.5mm$
- For +x reinforcement $z^T = d'' - \frac{y^T}{2} = 254 - \frac{10.48}{2} = 248.76mm$
- For -x reinforcement $z^T = d' - \frac{y^T}{2} - 28 = 270 - \frac{12.62}{2} - 28 = 229.37mm$

5. Moment resisting capacity during fire (Mrd)

   we can evaluate the new resisting moments for each fire condition using Equation 16.

- For +y reinforcement

$$m_{rd}{}^{T} = A_s.f_{yk}{}^{T}.Z^{T} = 2998 * 0.791 * 500 * 223.5 = 265.0\text{KNm/m}$$

- For +x reinforcement

$$m_{rd}{}^{T} = A_s.f_{yk}{}^{T}.Z^{T} = 267 * 1.0 * 500 * 248.76 = 33.210\text{KNm/m}$$

- For -x reinforcement

$$m_{rd}{}^{T} = A_s.f_{yk}{}^{T}.Z^{T} = 2998 * 1.0 * 500 * 229.37 = 73.858\text{KNm/m}$$

6. Ratio between moments

$$m^{+}{}_{x} = \lambda_1 m^{+}{}_{y} = 0.1253 m^{+}{}_{y}$$
$$m^{-}{}_{x} = \lambda_2 m^{+}{}_{y} = 0.2787 m^{+}{}_{y}$$
$$m^{-}{}_{y} = \lambda_3 m^{+}{}_{y} = 0.20 m^{+}{}_{y}$$

7. Position of the yield line .
   Using Equation 12 and 13;

α =0.5760, where ($\mathbf{0} < \alpha \leq 1$) ……. ok
β =0.633, where ($\mathbf{0} < \beta \leq 0.5$) …… $NOT\ ok$

   Thus, only case one should be considered!

8. Load carrying capacity

Finally, substituting the moment resistance in to the two cases of the yield line load carrying capacity equations, we can obtain the collapse load due fire condition.

$$P_{u,1} = \frac{6m^{+}{}_{y}\left[(\lambda_1 + \lambda_2).\frac{b}{\alpha a}.+4\frac{a}{b}\right]}{a.b(3-\alpha)} = \frac{45.2382KN}{m2}/m$$

For the other fire duration, the results and plots are given below.

Temp.	Temp. Bars (°c)		Ks(θ)		kc(θ)	position of
	x	y	x	y		500°c isothermal lines(mm)
Tamb	20	20	1.00	1.000	1.00	0
R30	140	230	1.00	1.000	0.93	10
R60	260	385	1.00	1.000	0.77	22
R90	360	495	1.00	0.791	0.608	28
R120	440	565	0.912	0.578	0.502	36
R180	550	670	0.625	0.302	0.345	48
R240	600	745	0.47	0.176	0.24	60
R300	650	800	0.35	0.110	0.15	67

Table:5 Positions of 500°C isothermal lines and strength reduction coefficients.

							Unltimate load			
Temp.	Internal lever arm (zT)			Limit moment (Mfire)			case 1		case 2	
	x+	y+	x-	x+	y+	x-	α	qu1	β	qu2
Tamb	248.76	211.22	257.37	33.210	316.612	82.874	0.5549694	52.95099	0.643811	53.8514
R30	248.76	211.22	247.37	33.210	316.612	79.654	0.5489564	52.65343	0.645226	53.82219
R60	248.76	211.22	235.37	33.210	316.612	75.790	0.5415688	52.29682	0.646939	53.78738
R90	248.76	223.50	229.37	33.210	265.008	73.858	0.5760382	45.23882	0.633305	45.2673
R120	249.23	236.02	221.37	30.344	204.495	71.282	0.622572	36.69116	0.616098	35.20887
R180	250.73	252.25	209.37	20.920	114.192	67.418	0.7284074	23.57213	0.579721	20.07236
R240	251.54	259.65	197.37	15.783	68.503	63.554	0.8303137	16.89999	0.540104	12.39588
R300	252.17	263.53	190.37	11.783	43.454	61.300	0.926189	13.29757	0.501444	8.147623

Table:6 Ultimate Load of the slab for different fire duration

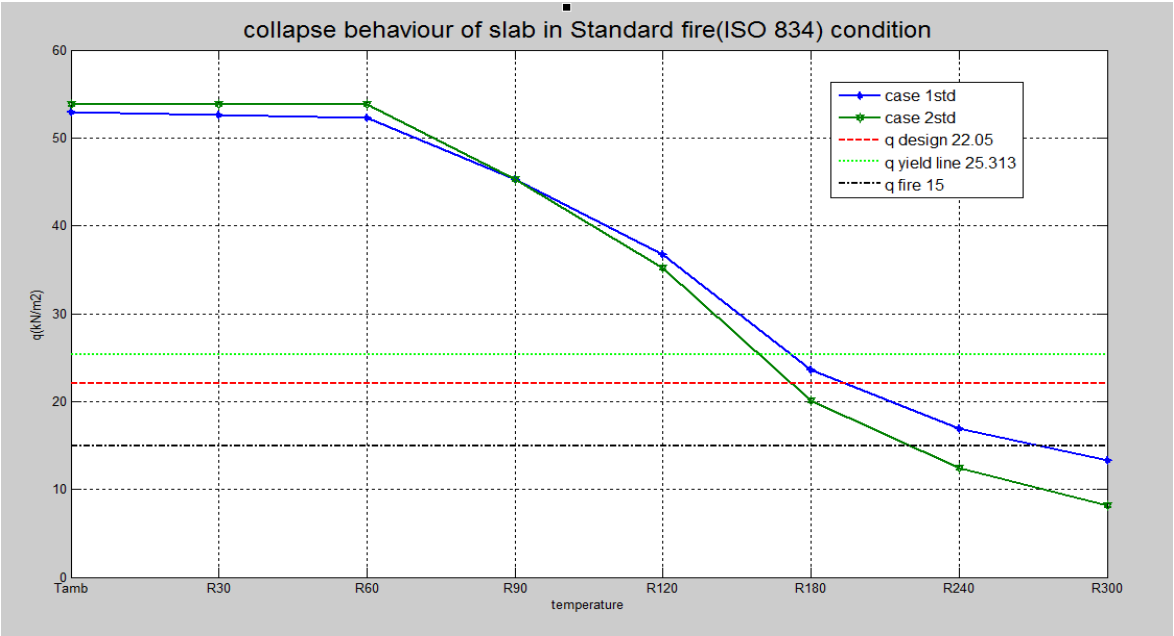

Figure 25:collapse load of the slab in standard fire condition, both cases.

From the table results, we can clearly observe that, the value of "β" is beyond the limit value

(0< β<0.5) which is not theoriticaly acceptable. Thus, for the given standard fire condition, the behaviour of the yield lines follows only case one. Thefore, the resistance of the slab for this fire condition as shown in figure 26 below, collapse occours at a fire duration, 275min, when the load resistance is lower than the design value.

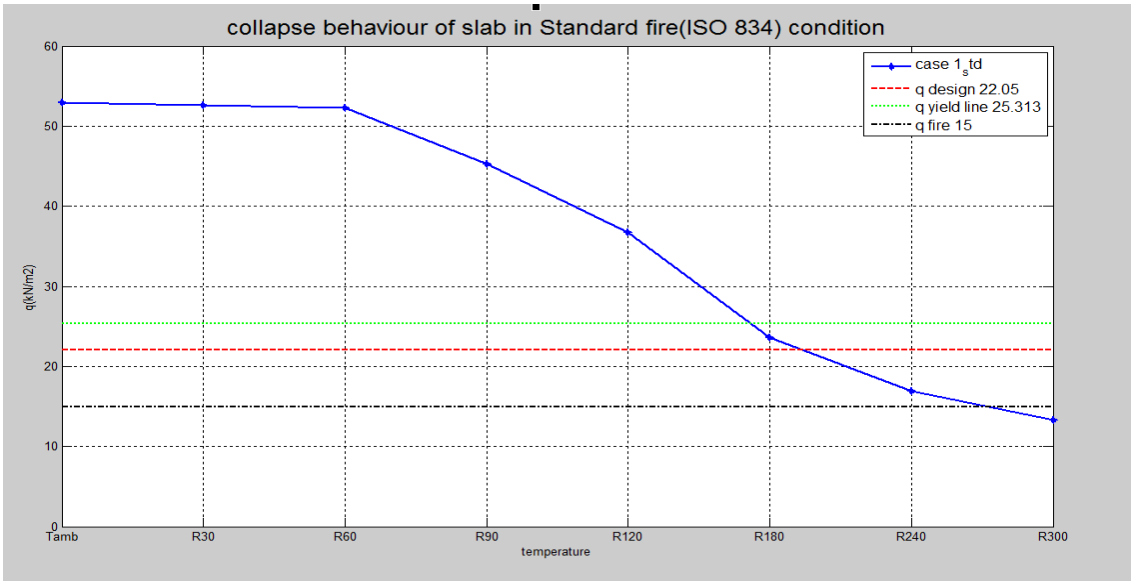

Figure 26: Actual collapse load of the slab in standard fire condition, only case 1.

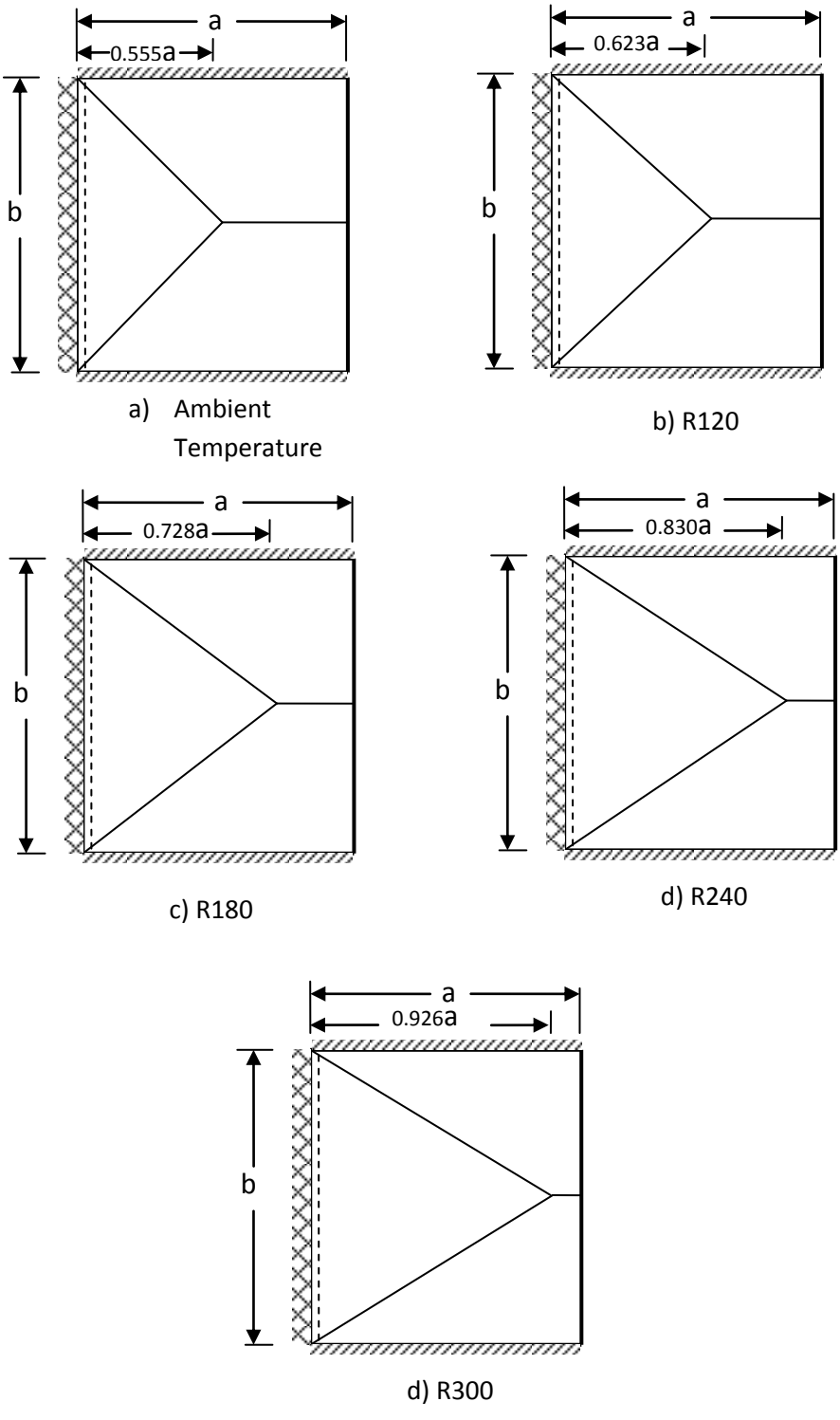

Figure 27: Evolution of mechanism 1 for different fire durations (ISO 834)

Chapter 7

REAL FIRE SCENARIO CALCULATION FOR THE SLAB

7.1 Boundary conditions

The boundary conditions of the library room considered in this paper are as follows:

- NO automatic fire suppression
- NO independent water supplies
- NO automatic detection and alarm systems, either by heat or smoke
- NO automatic transmission to fire brigade
- NO smoke exhaust system
- The library is provided with safe access routes
- The library is provided with fire-fighting devices

The designed fire load density is obtained from an expression from EN 1991-1-2 which takes into account the characteristic fire load depending from occupancy of building, combustion, compartment area, type of occupancy and the effect of active fire fighting measures as:

$$q_{f,d} = q_{f,k}.m.\delta_{q1}.\delta_{q2}.\delta_{n} \quad \text{(Eq.17)}$$

where:

- $q_{f,k}$ characteristic fire load density.
- m combustion factor which is in function of type fire load, ***m=0.8 for cellulosic fire***
- $\delta_{q,1}$ consider the compartment size
- $\delta_{q,2}$ consider the type of occupancy
- δ_{n} factors which considers the effect of the active fire fighting measures

Fire Load Density.

Fire load density q_{fk} is the fire load per unit area related to the floor area. Data are available for different types of occupancies of compartments (EN 1991-1-2, 2002). In order to obtain these data, the mass off all types of combustible present in compartment is measured or estimated. This mass is then multiplied by the combustion heat of the materials that constitutes the fire load. This quantity is then divided by the floor area of the compartment, according to Eq.(18)

$$q_{f,net} = \frac{1}{A_f}\sum_i H_{c,i}\, M_i \ldots\ldots\ldots\ldots\ldots\ldots \text{(Eq. 18)}$$

$q_{f,k}$ ***=1824 MJ/m²*** was chosen from table below for library room occupancy.

Occupancy	Average	80% Fractile
Dwelling	780	948
Hospital (room)	230	280
Hotel (room)	310	377
Library	1 500	1 824
Office	420	511
Classroom of a school	285	347
Shopping centre	600	730
Theatre (cinema)	300	365
Transport (public space)	100	122
NOTE Gumbel distribution is assumed for the 80 % fractile.		

$\delta_{q,1}$ ***=1.33*** for area ***A=96 m²*** found by interpolation from the table below

Compartment floor area A_f [m²]	Danger of Fire Activation δ_{q1}
25	1,10
250	1,50
2 500	1,90
5 000	2,00
10 000	2,13

$\delta_{1,2}=1$ from type of occupancy (office type..library) from the table below

Danger of Fire Activation δ_{q2}	Examples of Occupancies
0,78	artgallery, museum, swimming pool
1,00	offices,residence, hotel, paper industry
1,22	manufactory for machinery & engines
1,44	chemical laboratory, painting workshop
1,66	manufactory of fireworks or paints

Active control

Active control refers to control of the fire by some actions taken by the person or an automatic devices and apply fire protection measures. These systems usually employ an extinguishing that is used at a time of fire incidents. common systems include fire hydrants, monitors, hose reel for manual application and automatic sprinklers. Automatic fire extinguishing systems are usually arranged in combination with detection and control systems.

δ_{ni} Function of Active Fire Fighting Measures									
Automatic Fire Suppression		Automatic Fire Detection			Manual Fire Suppression				
Automatic Water Extinguishing System	Independent Water Supplies	Automatic fire Detection & Alarm		Automatic Alarm Transmission to Fire Brigade	Work Fire Brigade	Off Site Fire Brigade	Safe Access Routes	Fire Fighting Devices	Smoke Exhaust System
	0 | 1 | 2	by Heat	by Smoke						
δ_{n1}	δ_{n2}	δ_{n3}	δ_{n4}	δ_{n5}	δ_{n6}	δ_{n7}	δ_{n8}	δ_{n9}	δ_{n10}
0,61	1,0 | 0,87 | 0,7	0,87 or 0,73		0,87	0,61 or 0,78		0,9 or 1 or 1,5	1,0 or 1,5	1,0 or 1,5

Table:7 Functions of active fire measure factors.

Equation below gives the Multiplicative sum as:

$$\delta_n = \prod_{i=1}^{10} \delta_{ni} \text{.....(Eq. 19)}$$

Hence from equation (Eq.19) and the table we obtain that:

$$\delta_n = 1.17$$

For the normal fire fighting measures, which should almost always be present, such as the safe access routes, fire fighting devices, and smoke exhaust systems in staircases, the δ_{ni} values of Table above should be taken as 1,0. However, if these fire fighting measures have not been foreseen, the corresponding δ_{ni} value should be taken as 1.5.

Automatic Fire Suppression (**yes**, **no**)	**no**	1.00
Independent Water Supplies (**0**, **1**, **2**)	**0**	1.00
Autom Detect & Alarm by **heat** (**yes**, **no**)	**no**	1.00
Autom Detect & Alarm by **smoke** (**yes**, **no**)	**no**	1.00
Aut Alarm Transm to Fire Brigade (**yes**, **no**)	**no**	1.00
On site Fire Brigade (**yes**, **no**)	**no**	
Off Site Fire Brigade (**yes**, **no**)	**yes**	0.78
Safe Access Routes (**yes**, **no**)	**yes**	1.00
Fire Fighting Devices (**yes**, **no**)	**yes**	1.00
Smoke Exhaust System (**yes**, **no**)	**no**	1.5

Table:8 Fire fighting measures

From equation17, the designed fire load is:

$$q_{f,d} = 2276 \frac{MJ}{m^2}$$

$$q_{t,d} = q_{f,d} * \frac{A_f}{A_t} \text{.....(Eq.20)}$$

which is design fire load reduced by ratio between floor area and enclosure are (walls, floor and ceiling)

$$q_{t,d} = 2276 * \frac{96}{332} = 658.12 \frac{MJ}{m^2}$$

Opening factor

The amount of ventilation in a fire compartment is often described by the ventilation factor or opening factor given by:

$$o = (A_v\sqrt{h_v})/A_t \text{.....(Eq.21)}$$

$$o = \frac{9\sqrt{1.5}}{332} = 0.033$$

total area of vertical openings	A_v =	9	m^2
average height of the openings	h_v =	1.5	m
total area of the enclosure	A_t =	332	m^2

Evaluation of thermal inertia

All building designs which have to take account of energy conservation consider then effect of thermal inertia of the building materials in order to minimize the transmission of heat through building elements. However, calculation takes into account only thermal insulation of the building assuming the steady-condition, which doesn't always occur in practice (RILM recommended practice, 2005).

The mass of the building's roof, walls and floors influences the rate of heat transmission. The larger the mass the longer it takes to heat up the inside part of the structure. Other factors such as, the thermal conductivity, the specific heat and density of the building elements, also play an important role. For the purpose of comparing various walls and roof elements the thermal inertia is given as ($b = \sqrt{\rho.c.\lambda}$). A higher thermal inertia will result in a low heat transmission and vise versa.

b factor - thermal inertia						
	area(m^2)	ρ (kg/m^3)	c	λ (W/m°C)	b_i	$b_i \cdot A_i$
walls	131	1012	882	0.3	519	67789
floor	**96**	1012	882	0.3	519	49677
ceiling	96	1012	882	0.3	519	49677
Total	**323**				**519**	167143
(openings excluded)					W $s^{1/2}$ / m^2°C	

Evaluation of time factor function.

$$\Gamma = \left(\frac{O}{0.04} \Big/ \frac{b}{1160} \right)^2 = \left(\frac{0.033}{0.04} \Big/ \frac{512}{1160} \right)^2 = 3.44 \ldots\ldots\ldots\ldots\ldots\ldots\ldots\ldots\ldots (\text{Eq. } 22)$$

The shortest possible duration of the heating phase t_{lmi}=*15 min*

Depends on the fire growth rate (slow, medium, fast) t_{lim} = 25, 20,15 minutes

t_{lmi}=15 min *is the minimum duration of the heating phase because of the fuel controlled kinetics of flames*

Duration of the ventilation-controlled heating phase t_{max}

During fire, the rate of temperature rise vary with time. In order to estimate the duration of fire, the relationship between the fire load and the opening must be considered. The maximum temperature in the heating phase occurs at a time t_{max} given by equation below.

$$t_{max} = (0.2 * 10^{-3} q_{t,d})/O \ldots\ldots\ldots\ldots\ldots\ldots\ldots\ldots\ldots (\text{Eq. } 23)$$

t_{max}=3.964 h *is the time needed to reach the maximum temperature, that is the maximum between the ventilation controlled time to burn the fire load (Kawagoe's formula) and the fuel controlled minimum time t_{lim}*

Fictitious time t*

$$t_{\max}{}^{*} = \Gamma \cdot t_{\max}$$

t_{max}*=13.636 h *is the fictitious time to reach the maximum temperature.*

It is obtained via the pertinent time scale factor Γ *or* Γ_{lim} *for ventilation and fuel-controlled fires respectively.*

The maximum temperature is T_{max}=1317^{0}C

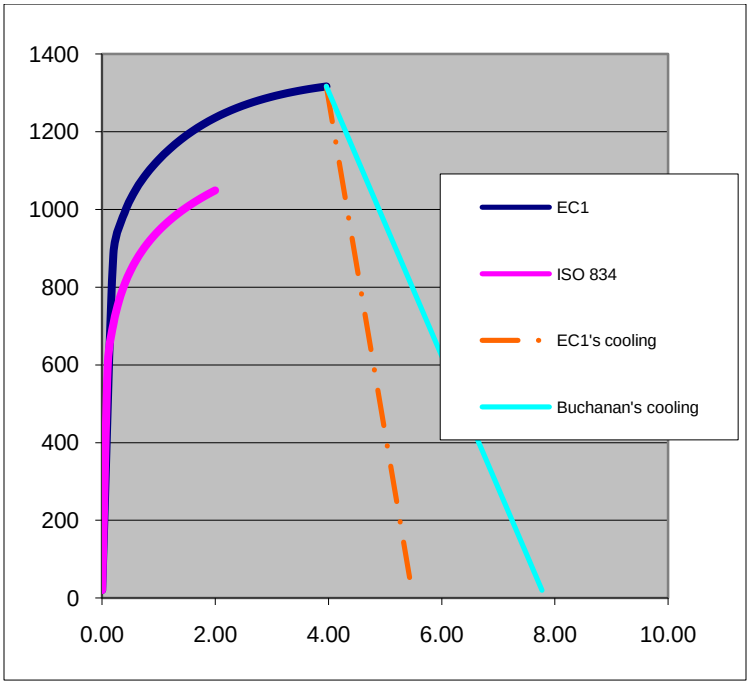

Figure 28: Time temperature curve. Y is the temperature (^{0}C) and X is the time (h)

7.2 Analysis Results from ABAQUS.

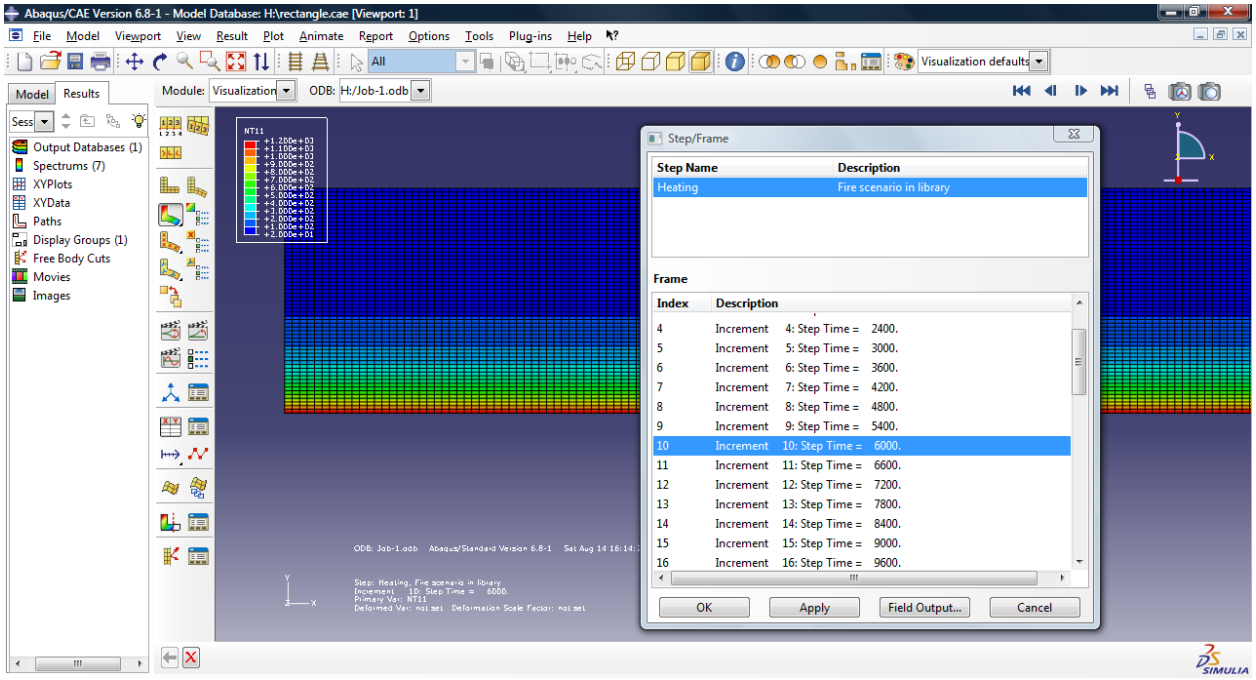

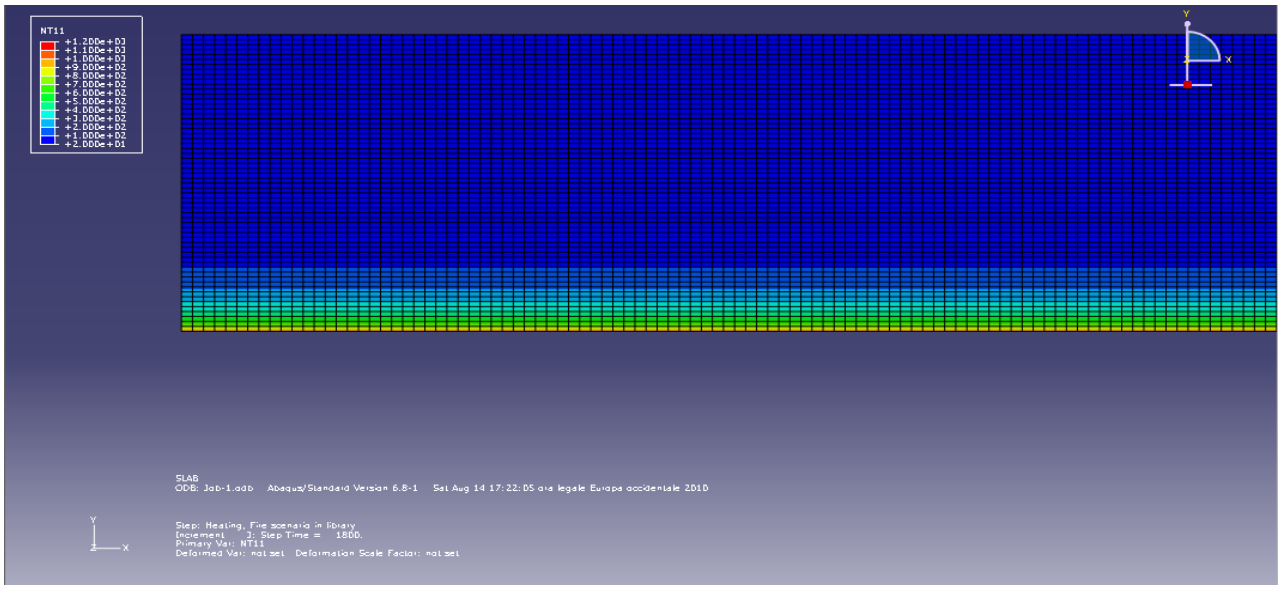

Result after 30min.

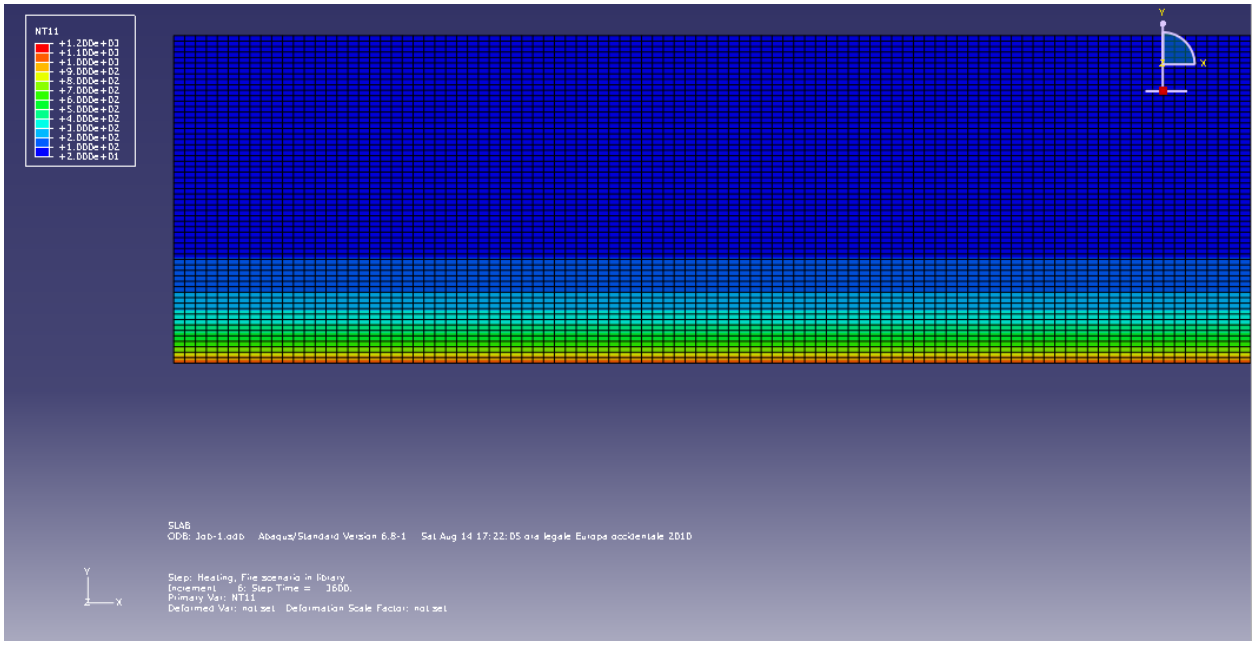

Result after 60min.

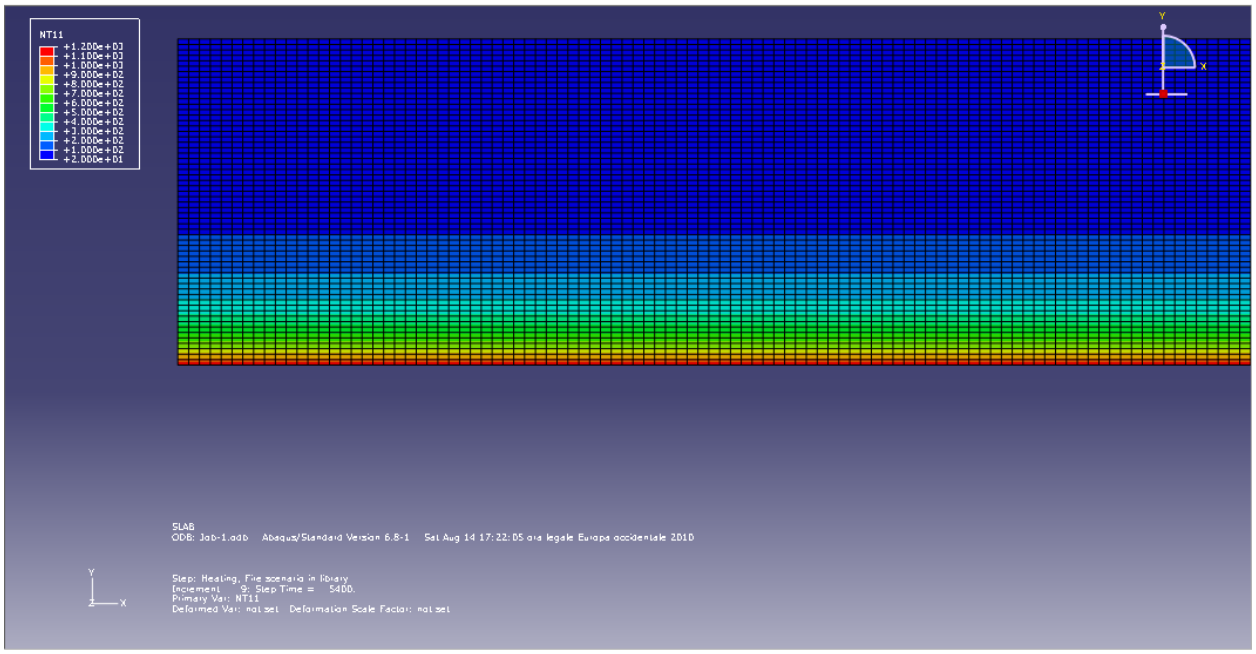

Result after 90min.

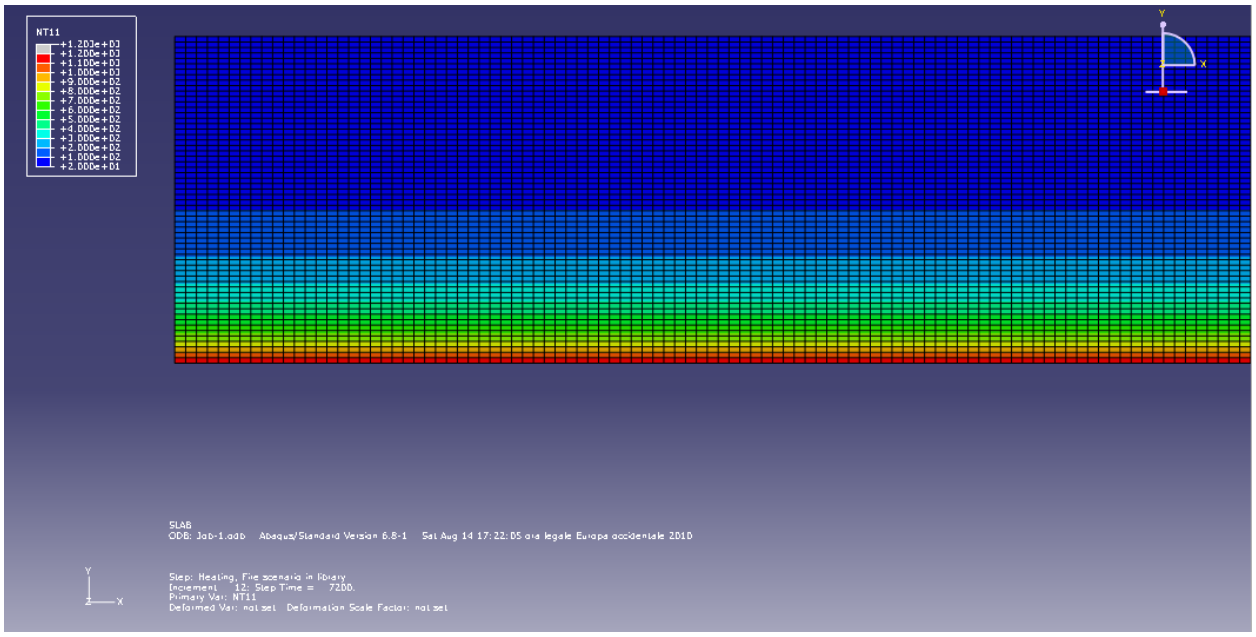

Result after 120min.

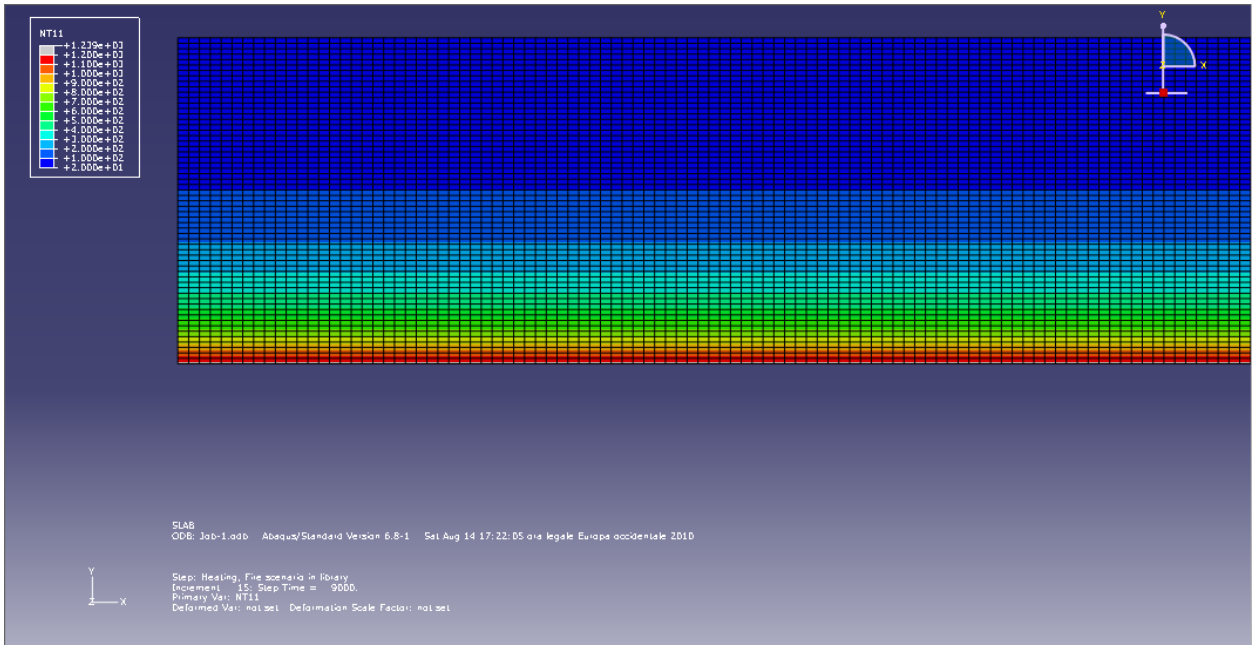

Result after 150min.

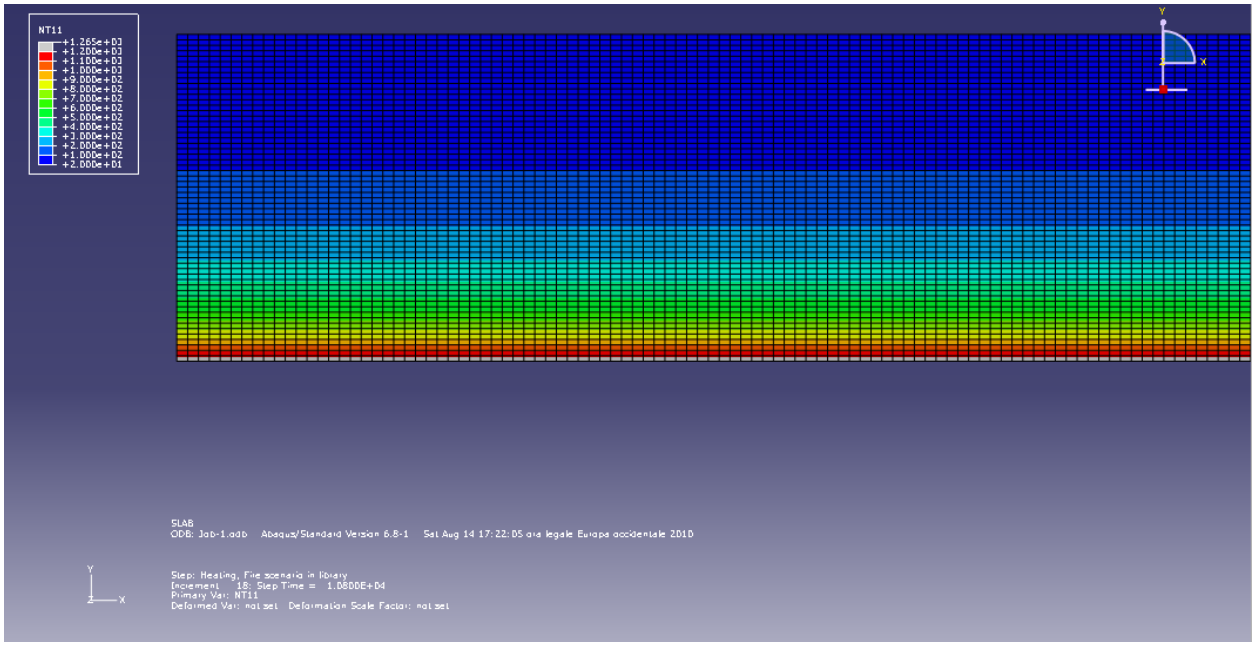

Result after 180min.

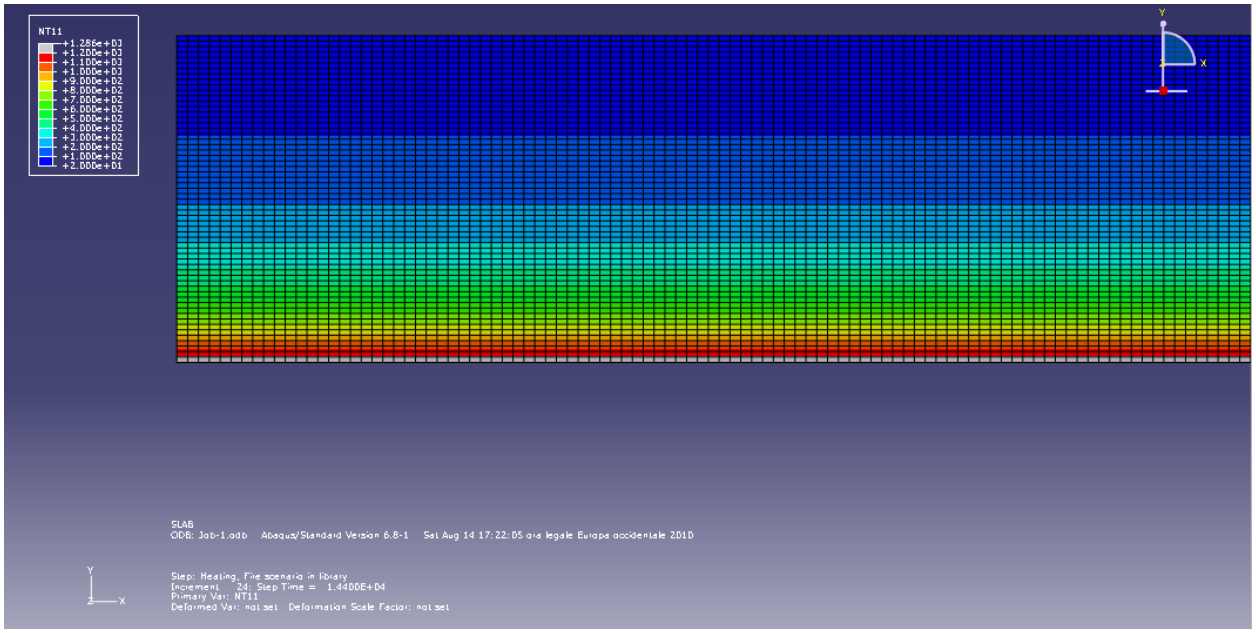

Result after 240min.

Similarly as done for the standard fire, we read the 500°C isothermal lines from the ABAQUS and read the corresponding reinforcement temperature for different fire duration, as well as the strength reduction coefficients.

Temp.	Temp. Bars (°c)		Ks(θ)		kc(θ)	position of
	x	y	x	y		500°c isothermal lines(mm)
Tamb	20	20	1.00	1.000	1.00	0
R30	210	300	1.00	1.000	0.85	16
R60	320	430	1.00	0.934	0.705	27
R90	420	620	0.96	0.426	0.42	37
R120	510	670	0.749	0.316	0.345	45
R150	550	730	0.625	0.194	0.255	53
R180	600	780	0.47	0.134	0.18	58
R240	690	860	0.272	0.080	0.108	69
R300	750	920	0.175	0.056	0.07	75

Table:9 Positions of 500°C isothermal lines and strength reduction coefficients for real fire scenario.

Temp.	Internal lever arm (zT)			Limit moment (Mfire)			case 1		case 2	
	x+	y+	x-	x+	y+	x-	α	qu1	β	qu2
Tamb	248.765	211.216	257.373	33.210	316.612	82.874	0.555	52.951	0.644	53.851
R30	248.765	211.216	241.373	33.210	316.612	77.722	0.545	52.475	0.646	53.805
R60	248.765	215.095	230.373	33.210	301.148	74.180	0.549	50.085	0.644	51.223
R90	248.995	244.958	220.373	31.778	156.424	70.960	0.688	30.474	0.587	27.366
R120	250.079	251.424	212.373	25.006	119.096	68.384	0.732	24.711	0.574	21.015
R150	250.728	258.596	204.373	20.920	75.201	65.808	0.829	18.513	0.534	13.680
R180	251.539	262.123	199.373	15.783	52.652	64.198	0.900	15.116	0.507	9.810
R240	252.576	265.297	188.373	9.172	31.814	60.656	0.994	11.712	0.474	6.150
R300	253.105	266.767	181.373	5.778	21.994	58.402	1.064	8.450	0.446	4.406

Table:10 Ultimate Load of the slab for different fire duration.

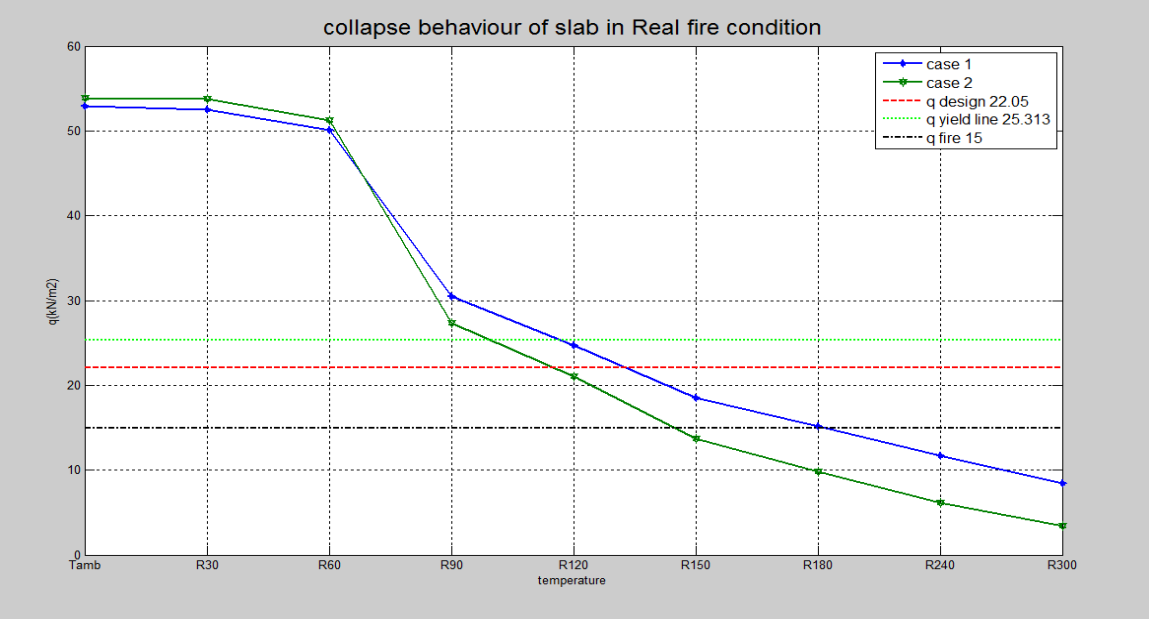

Figure 29: Collapse load of the slab in real fire condition, both cases.

Similarly from the table results, we can clearly observe that, the value of "β" is beyond the limit value $(0< \beta<0.5)$ which is not theoriticaly acceptable. Thus, for the given real fire condition, the behaviour of the yield lines follows only case one before the collapse. Thefore, the resistance of the slab for this fire condition as shown in figure 30 below, collapse occours at a fire duration, 180min when the load resistance is lower than the deisgn value.

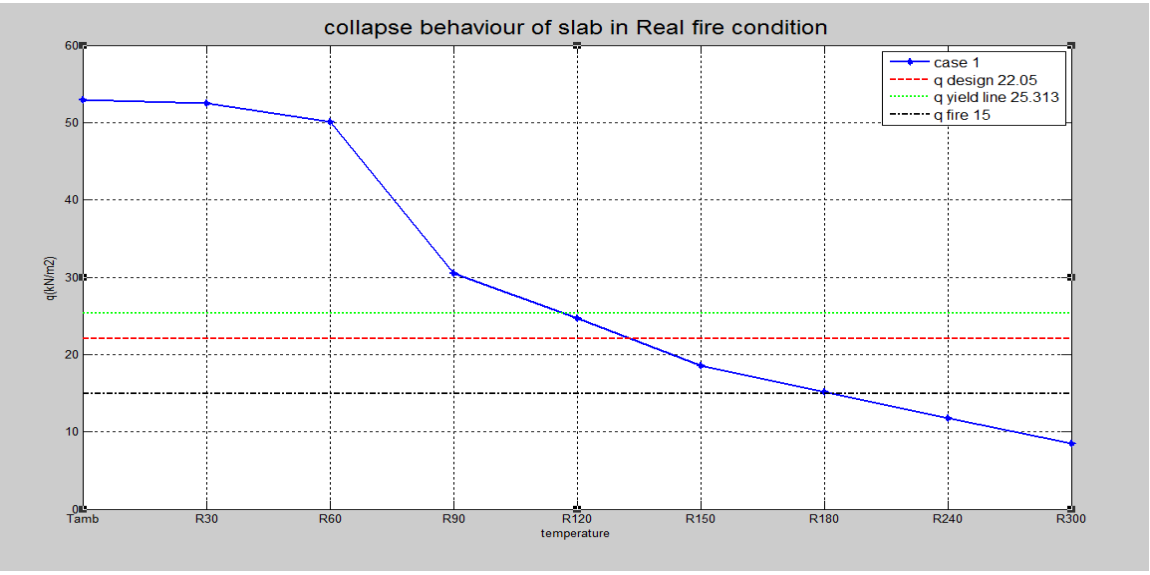

Figure 30: Collapse load of the slab in real fire condition, only case 1.

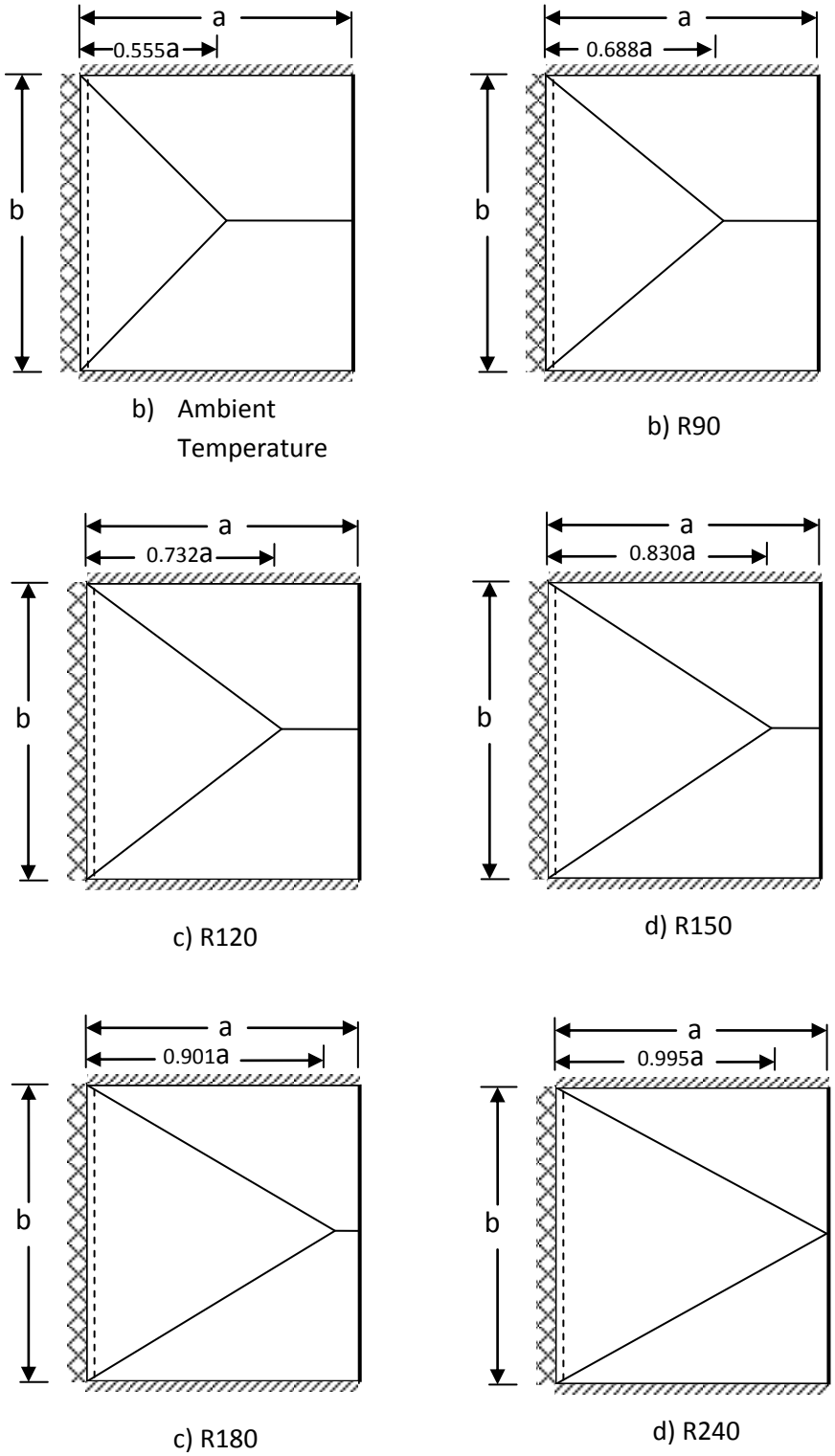

Figure 31: Evolution of mechanism 1 for different real fire durations.

Evolution of mechanism two in real fire condition.

Even though the slab would collapse for the given strength and material properties at 180min in the real fire scenario, it will be interesting to observe how the yield-line mechanisms could change after a time of 180min from mechanism one to two if the slab had enough strength for further fire duration.

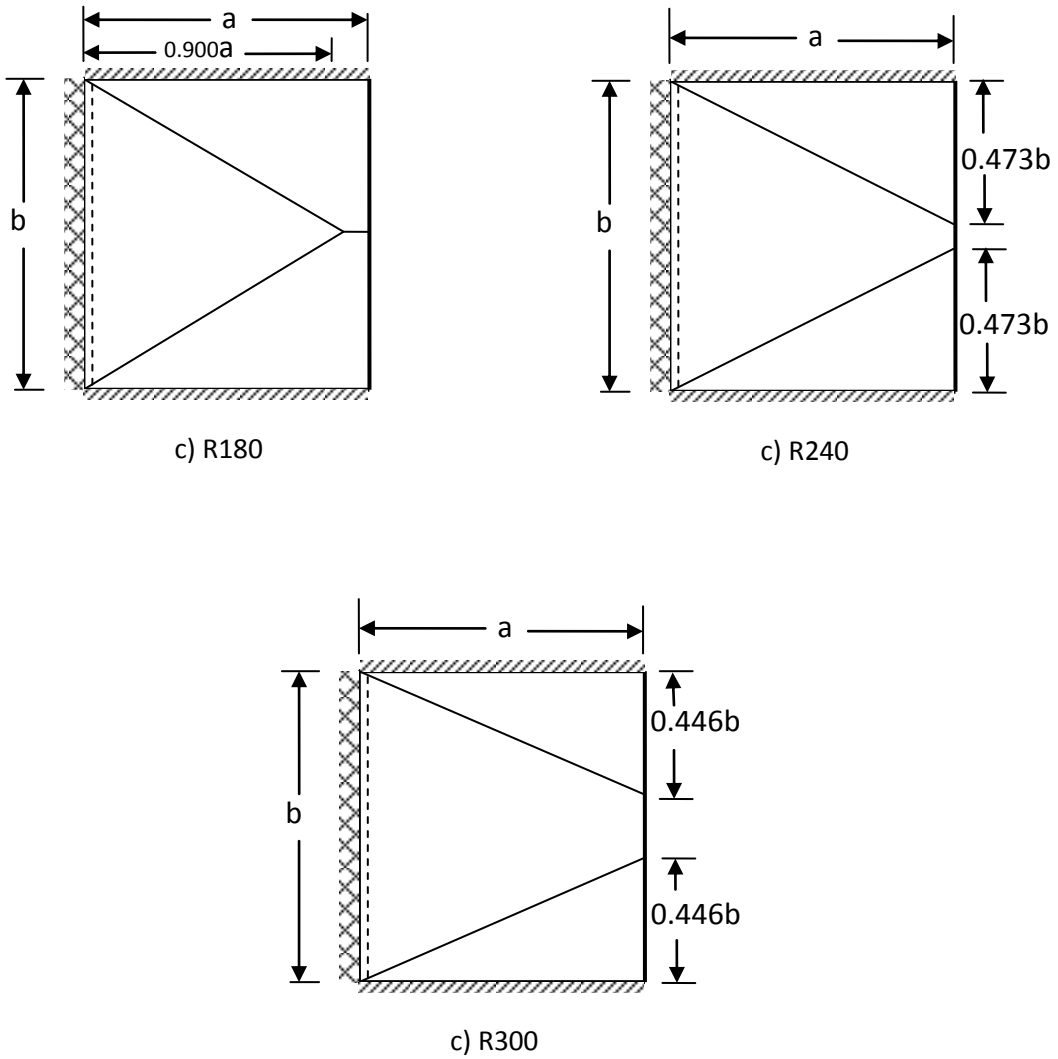

Figure 32: Evolution of mechanism 2 after R180 in real fire condition.

7.3 DESIGN AND DETAIL CONSIDERATIONS

Bond

This is generally not a problem even though bond strengths are severely reduced in a fire. The problem is more likely to be worst in pre-stressed concrete construction where bond in the anchorage length is needed to transfer the pre-stress force into the concrete. It is not a general practice to check bond strength in fire design.

Spalling

Spalling occurs in one of two forms in fire. The first is explosive spalling which occurs very early in a fire and likely lead to loss of cover to the main reinforcement and hence to more rapid rise in temperature and resultant strength loss leading to reduced fire performance. The second form is known as sloughing, whereby the concrete gradually comes away due to loss of effective bond and strength loss. This mode tends to occur toward the end of fire and rarely critical.

The exact mechanism of explosive spalling is still not understood, but it is affected by the following factors (Malhotra, 1984; Connolly, 1997; John A. Purkiss, 2007)

- Moisture content

A concrete with a high moisture content is more likely to spall since one of the possible mechanisms of spalling is due to the buildup of high vapour pressure near the surface causing tensile failures in concrete caused by moisture clog. However, it is now recognized that the critical isotherm for pore pressure buildup is the 200°C isotherm and not the 100°C(Khalafallah, 2001). The blanket limit of a moisture content of 3%, below which EN 1992-1-2 indicates spalling will not occur.

- Concrete porosity and permeability

A more porous concrete, and therefore one with a high permeability, will allow the dissipation of vapour pressure, and thus relieve any buildup within the concrete section. However, it must be pointed out that a porous concrete will give poor performance with respect to durability. It has also become clear that it is a combination of moisture content and permeability is critical (Tencheve and Purnell, 2005)

- Aggregate type

The evidence available suggests that the aggregate most likely to give spalling is siliceous aggregate, with limestone producing less spalling and lightweight concrete the least. This is likely to be linked to the basic porosity of the aggregate, in that siliceous aggregate is impermeable compared to the others and that moisture transport has to occur thorough the mortar matrix.

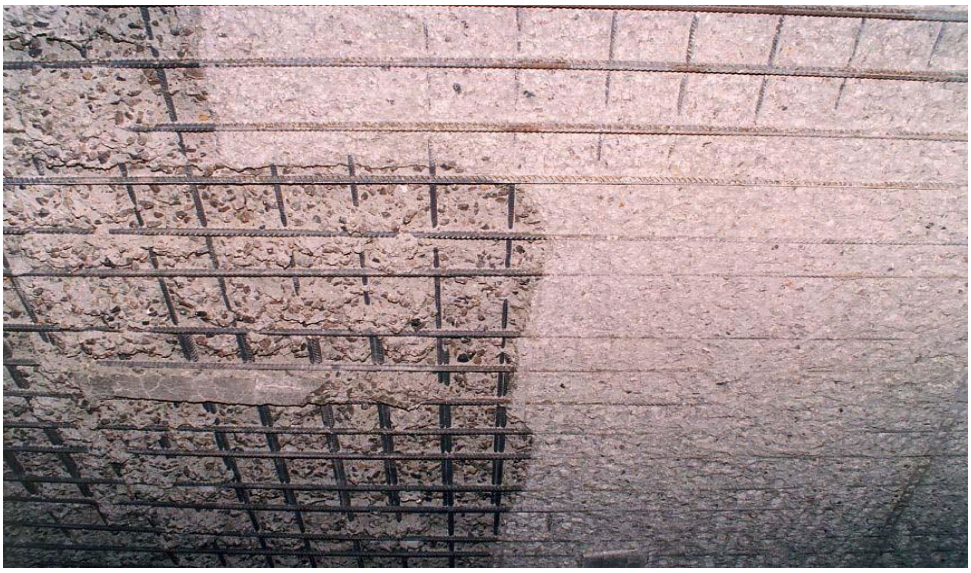

Fig:32 Spalling (expulsion) of the cover.

- Section profile and cover

There is some evidence to suggest that sharp profiles will produce more spalling than rounded edges. High covers are also likely to produce greater amounts of spalling. Thus design codes frequently place restrictions when high cover are needed at high fire resistance period in order to maintain low temperature at the reinforcements inside (EN 1992-1-2).

- Heating rate

The higher the heat flux, the less the chance pore pressures have to dissipate to the relatively cool regions of a concrete element. The rate of heating is therefore critical for the spalling phenomenon.

Chapter 8

CONCLUSIONS AND RECOMMENDATIONS

The method presented here for the analysis and design of reinforced concrete slabs using the *strip method* proposed by A. Hillerborg gives, as we have seen, lower bound values for the collapse loads of slabs. However, in relatively simple cases of slab geometry and loading, the *yield-line method* can be used as a design method since the fracture pattern can be obtained with reasonable accuracy.

It should also be noted that a complete elastoplastic analysis is generally quite complicated. The complexities arise mainly from the necessity of carrying out an analysis in an iterative and incremental manner. The development of efficient alternative methods can be used to obtain the collapse load of a structural problem in a simple and more direct manner without recourse to an iterative and incremental analysis is, therefore, of great value to practicing engineers, despite the fact that the information so obtained is just a part of the total solution.

Thus, Limit-analysis is concerned with the development and applications of such methods that can furnish the estimation of collapse load of a structure in a direct manner. The estimation of the collapse load is of great value, not only as a simple check for a more refined analysis, but also as a basis for engineering design.

It should be emphasized here that the collapse load as calculated in limit analysis is different from the actual plastic collapse load, as it occurs in a real structure or body. Herein, we calculated the collapse load of an ideal structure, at which the deformation of the structure can increase without limit while the load is held constant. This, of course, rarely happens in a real structure, and hence, the limit analysis calculations apply strictly, not to real structures, but to idealized one. Nevertheless, a load computed on the basis of this definition or idealization may give a good approximation to the actual plastic collapse load of a real structure.

Also, in practice the actual collapse load of a slab may be above the calculated value because of secondary effects such as the kinking of the reinforcing steel in the vicinity of the fracture line and the effect of horizontal edge restraints which induce high compressive forces in the plane of the slab with a consequent increase in load capacity.

Glossary

Active fire control: control of the fire by some actions taken by the person or an automatic devices and apply fire protection measures

Compartment fire: a fire which remain confined in the compartment.

Design fire: a specified fire development for deign purposes.

Design fire fuel density: the fire load density considered for determining thermal actions in fire design.

Design fire scenario: a specific fire scenario on which analysis will be conducted.

Enclosure: used as synonym of fire compartment

Euro code: within an action programme, the commission of European community, took the initiative to establish a set of harmonized technical rules for the design of construction works. These harmonized technical rules are gathered in a set of documents called the Euro Code

The Structural Eurocode document comprises the following standards generally consisting of a number of Parts:

- EN 1990 Eurocode : Basis of Structural Design
- EN 1991 Eurocode 1: Actions on structures
- EN 1992 Eurocode 2: Design of concrete structures
- EN 1993 Eurocode 3: Design of steel structures
- EN 1994 Eurocode 4: Design of composite steel and concrete structures
- EN 1995 Eurocode 5: Design of timber structures
- EN 1996 Euro code 6: Design of masonry structures
- EN 1997 Euro code 7: Geotechnical design
- EN 1998 Euro code 8: Design of structures for earthquake resistance
- EN 1999 Euro code 9: Design of aluminium structures

Fire load: the sum of thermal energies which are released by the combustion of all combustible materials in the building (building contents and construction materials).

Fire load density: the fire load per unit area related to the floor area.

Fire resistance: the ability of a structure, a part of a structure or a member to fulfill its required functions, for specified load level, for specified fire exposure and for specified period of time.

Flashover: simultaneous ignition of all the fire loads in the compartment.

Fully developed fire: the state of full involvement of all combustible surfaces in a fire within a specified space.

Ignition of the fire: the first step of any compartment fire: without ignition no fire.

Localized fire: a fire involving only a limited area of the fire load in the compartment.

Member: a basic part of a structure (such as beams, column etc.)

Opening factor: factor representing the amount of ventilation depending on the area of the openings in the compartment walls, on the height of these openings and on the total area of enclosures surfaces.

Pre-flashover fire phase: fire phase before simultaneous ignition of all fire loads in a compartment.

Post-flashover fire phase: fire phase after simultaneous ignition of all fire loads in a compartment.

Rate of heat release: heat(energy) released by all combustible materials in the compartment as function of time.

Standard fire resistance: the ability of a structure or part of it to fulfill the required functions (load-bearing function and or Integrity function), for the exposure of heating for specified load combination and for specified period of time.

Temperature-time curves: temperature in the environments of member surfaces as a function of time. They may be:

- Conventional curves adopted for classification or verification of fire resistance, e.g. the standard temperature-time curve, external fire curves, hydrocarbon fire curves.
- Parametric: determined on the basis of fire models and the specific physical parameters defining the conditions in the compartment.

Ventilation factor: factor representing the amount of ventilation depending on the area of the openings in the compartment walls and on the height of these openings.

References

1. Arne Hillerborg, 1996: *Strip Method Design Handbook:* E & FN Spon, an imprint of Chapman & Hall, London, UK.
2. Adam Levesque, 2006. *Fire Performance of Reinforced Concrete Slabs*: Worcester Polytechnic Institute.
3. Buchanan, A. H. (2001). *Structural Design for Fire Safety*. Chichester: John Wiley & Sons Ltd
4. Dr. Colin Caprani, 2006/7. *Analysis and Design of slabs.*
5. D. Moore, T. Lennon, Y. Wang, 2007. *Designers' guide to EN 1991-1-2, EN 1993-1-2 and EN 1994-1-2*: Thomas Telford Ltd.
6. S.S RAY,1995. *Reinforced concrete, Analysis and design:* Blackwell science Ltd.
7. Pietro G. Gambarova, Dario Coronelli, Patrick Bamonte: 2007. *LINEE GUIDA PER LA PROGETTAZIONE DELLE PIASTRE IN C.A.*
8. Mario Monotti, 2004. *Reinforced Concrete slab-Compatibility Limit Design.*ETH Zurich.
9. M.P. Nielsen, 1999. *Limit Analysis and Concrete Plasticity*: John Wiley & Sons Ltd.
10. Joost Meyboom,(2002). *Limit Analysis of Reinforced Concrete slabs*. ETH Zurich.
11. Malhotra, H. L. (1982). Design of Fire-Resisting Structures. Bishopbriggs and Glasgow: Surrey University Press.
12. EN1990, EN 1991, EN1992
13. Lie, T. T. (Eds.) (1992). *Structural Fire Protection*. New York: American Society of Civil Engineers

14. Knud Winstrup Johansen, 2002. *Yield-Line Formulae for Slabs:* Cement and concrete Association, London.
15. Robert J. Cope, L.A. Clark, 1984. *Concrete Slab: Analysis and Design*: Elsevier Applied Science publisher Ltd.
16. Robert Park, William Leo Gamble, 2000. *Reinforced Concrete Slabs*: John Wiley & Sons Ltd.
17. S. Aroni, RILEM Technical Committee 78-MCA., RILEM Technical Committee 51-ALC
18. John A. Purkiss, 2007. *Fire safety engineering design of structures*: Elsevier Applied Science publisher Ltd.
19. Wai-Fah Chen, 2007. *Plasticity in reinforced concrete*: McGraw-Hill, NewYork.
20. T. Z. Harmathy, 1985 *Fir safety, science and engineering: a symposium*, ASTM Committee E-5 on Fire Standards, Society of Fire Protection Engineers.
21. Jean-Francois Cadorni, 2003. *Compartment fire Model for structural Engineering*, Doctorial thesis, Universitè de liege.
22. Wade, C. (1991). *Method for fire engineering design of structural concrete beams and floor systems.* Judgeford: BRANZ, The Resource Centre for Building Excellence